

## A MODEL DESCRIBING THE GROWTH AND THE SIZE DISTRIBUTION OF MULTIPLE METASTATIC TUMORS

ANNE DEVYS, THIERRY GOUDON AND PAULINE LAFITTE

Equipe-Projet SIMPAF, Centre de Recherche INRIA Lille Nord Europe  
Parc Scientifique de la Haute Borne, 40, avenue Halley B.P. 70478  
F-59658 Villeneuve d'Ascq cedex, France

Laboratoire Paul Painlevé, UMR 8524  
CNRS–Université des Sciences et Technologies de Lille  
Cité Scientifique, F-59655 Villeneuve d'Ascq Cedex, France

(Communicated by Christian Schmeiser)

ABSTRACT. Cancer is one of the greatest killers in the world, particularly in western countries. A lot of the effort of the medical research is devoted to cancer and mathematical modeling must be considered as an additional tool for the physicians and biologists to understand cancer mechanisms and to determine the adapted treatments. Metastases make all the seriousness of cancer. In 2000, Iwata et al. [9] proposed a model which describes the evolution of an untreated metastatic tumors population. We provide here a mathematical analysis of this model which brings us to the determination of a Malthusian rate characterizing the exponential growth of the population. We provide as well a numerical analysis of the PDE given by the model.

**1. Introduction.** In this paper we are concerned with a mathematical model describing the growth of tumors. The model has the form of a PDE which looks like a conservation law, endowed with a boundary condition of non local type. Precisely, tumors are characterized by their size  $x \geq 1$  and we are concerned with the behavior of the size distribution  $\rho(t, x)$ :

$$\int_u^v \rho(t, x) dx$$

gives the number of tumors with size ranging in the domain  $[u, v]$  at time  $t \geq 0$ . The dynamics are governed by the combination of two phenomena:

- a tumor of size  $x$  grows with a rate  $w(x) \geq 0$ ,
- the growing tumor also emits new malignant cells with a rate  $\beta(x) \geq 0$ .

We further do not consider any treatment. Then, we are led to the following equation

$$\partial_t \rho + \partial_x (w\rho) = 0, \quad (1)$$

$$w(1)\rho(t, 1) = \int_1^\infty \beta(y)\rho(t, y) dy + \beta(x_p(t)). \quad (2)$$

---

2000 *Mathematics Subject Classification.* Primary: 35B40, 35Q80, 92C50, 65M99; Secondary: 35L50.

*Key words and phrases.* McKendrick-Von Foerster equation, relative entropy, asymptotic behavior, WENO scheme, metastatic tumors.

In (2), the last term accounts for the contribution of the primary tumor whose evolution follows the ODE

$$\frac{d}{dt}x_p(t) = w(x_p(t)), \quad x_p(0) = 1. \quad (3)$$

The problem is completed by assuming that initially there is no metastatic tumor

$$\rho|_{t=0} = 0. \quad (4)$$

The problem (1)-(4) appears exactly in that way in [9]. The model is intended to describe the earlier stages of the disease when the number of metastases remains far below measurement capabilities. Therefore the crucial point is to be able to characterize the large time asymptotics of the size distribution: we shall see that the main information is embodied into a positive parameter, that will be denoted  $\lambda_0$ , characterizing the speed of spread of the cancer at this stage. In fact we show that

$$\rho(t, x) \sim C e^{\lambda_0 t} N(x),$$

as  $t$  tends to infinity. Having a sharp estimate of this parameter, which depends on the functions  $w$  and  $\beta$ , is therefore particularly important to prevent tumour invasion and to devise successful treatment strategies. In addition to the introduction of the model, in [9], the solutions predicted by (1)-(4) are compared with size distributions successively measured by computed tomography images of a patient with hepatocellular carcinoma (liver cancer), showing the ability of the model to predict the tumors invasion.

System (1)-(4) belongs to the family of the so-called McKendrick-Von Foerster equations. Here, the assumptions on the coefficients are the following:

$$\begin{cases} w \in C^1(\mathbb{R}), \\ |w(x) - w(y)| \leq L|x - y|, \\ w(x) > 0 \text{ for any } x \in [1, b[, \quad w(b) = 0, \end{cases} \quad (5)$$

and for the emission rate we have

$$\beta \in L^\infty([1, b]), \quad \beta(x) > 0 \text{ on } [1, b] \quad (6)$$

The parameter  $1 < b < \infty$  represents the maximal size of a tumor: intuitively the larger the tumor, the more difficult it is to grow. In particular, the growth rate  $w$  vanishes at size  $b$ . As a consequence we note that

$$\int_1^b \frac{dx}{w(x)} = \infty. \quad (7)$$

Compared to classical McKendrick-Von Foerster models, where typically  $w = 1$ , this singularity induces non trivial difficulties in the mathematical analysis.

A typical model is given by the Gompertzian law

$$w(x) = ax \ln(b/x), \quad (8)$$

for some  $a > 0$  and then (3) can be integrated as follow:

$$x_p(t) = b^{1 - e^{-at}}. \quad (9)$$

The Gompertz law (1825) is an empirical one, but there exist biological models of the tumor growth which explain characteristic Gompertz-type growth curves. See [5, 8, 7, 10]. They are two-compartment models: they distinguish the proliferating cells and the quiescent ones. The behavior of these two types of cells and so the

inter-compartment transition rate function, depends on the tumor size. In [8], it is shown that in the case of a tumor forming a necrotic center the model predicts that the tumor grows monotonically to its ultimate size according to a typical S-shaped Gompertz' curve. We should specify that in those models the cells death is already taken in account.

The expression of the emission rate  $\beta$  depends on the distribution of blood to the tumors: current models are  $\beta(x) = m x^\alpha$ . When the tumor is vascular superficially, that is the blood vessels distribute on its surface,  $\alpha$  is assigned to  $2/3$  because the surface area of the tumor is proportional to  $x^{2/3}$ . On the other hand, when the blood vessel distribution is homogeneous in the tumor,  $\alpha$  is assigned to 1. In this paper,  $\alpha$  is dealt with as a parameter and for numerical simulations we adopt for  $\alpha$  the value obtained in [9] by comparison to clinical data ( $\alpha = 0.663$ ).

The mathematical questions we address here can be summarized as follows:

- the definition of the parameter  $\lambda_0 > 0$ , which in the population dynamics context would be interpreted as a Malthusian rate, relies on the resolution of an eigenvalue problem, associated to Equations (1)-(2). Usually exhibiting a solution to this problem combines the positivity and compactness properties of the underlying operator, through an application of the Krein-Rutman theorem [13]. However, the fact that  $w$  vanishes at some point introduces some singularity (see e.g. (7)), and leads to technical difficulties in applying such a method. Hence, we shall use a more direct approach, thanks to a tricky change of unknowns which simplifies the question. We obtain then the asymptotic behavior of the solution by an entropy method, see [12].
- the numerical simulation of the problem also presents some interesting difficulties since
  - the crucial question relies on a sharp evaluation of the asymptotic trend for large times and it thus requires some care in the numerical scheme we use;
  - the problem involves physical parameters ranging in an exponentially wide domain: in particular the typical value of  $b$  is very large ( $10^{11}$ ) which makes the use of reasonably refined meshes non affordable.

The paper is organized as follows. At first, we discuss some properties of the PDE (1)-(4). In particular, we establish the well-posedness of the problem under relevant conditions. We also show that the problem can be reinterpreted as a standard initial boundary value problem, without source term in the boundary condition. Secondly, we detail the corresponding eigenvalue problem. In turn, we discuss the large time asymptotics by using entropy methods, as presented in [11] and investigate the convergence rate. Finally, we describe how the problem can be handled numerically, so that we can compare on numerics the solution with the expected profile. It is worth mentioning that a similar program is addressed by D. Barbolosi, A. Benabdallah, F. Hubert and F. Verga [2] who use a completely different mathematical toolbox, both on the theoretical level where their proofs rely on semi-group arguments which yield very sharp results and on the numerical level since they use a different scheme based on characteristics (see also [1]). We add an Appendix with a discrete approach of the problem and show that (1)-(4) can be derived from a semi-discrete problem.

## 2. Analysis of the PDE.

**2.1. Existence and uniqueness of a solution.** Let us start by considering the evolution problem

$$\begin{cases} \partial_t f + \partial_x(wf) = 0, \\ f|_{t=0} = f_0, \end{cases} \quad (10)$$

where  $w$  fulfills (5). Since  $w$  has a positive value at  $x = 1$ , the problem (10) should be augmented with an incoming boundary condition

$$(wf)(t, 1) = k(t) \geq 0. \quad (11)$$

We aim at solving the initial-boundary-value problem (10)-(11).

To this end, we introduce the characteristics associated to  $w$ , that is the solutions of the autonomous ODE:

$$\frac{d}{dt}X(t, x) = w(X(t, x)), \quad X(0, x) = x. \quad (12)$$

We also set

$$J(-t, x) = \exp\left(-\int_{-t}^0 w'(X(\sigma, x)) d\sigma\right) = \exp\left(\int_0^t w'(X(-\sigma, x)) d\sigma\right), \quad (13)$$

which is the jacobian of the change of variable  $y = X(-t, x)$ , i.e.,  $dy = \partial_x X(-t, x) dx = J(-t, x) dx$ . Finally, we define the exit time function

$$T_*(x) = \inf\{t \geq 0, \text{ for any } 0 \leq s \leq t, X(-s, x) \in (1, b)\}.$$

In view of (5), we have  $X(-T_*(x), x) = 1$  when  $T_*(x)$  is finite. As a matter of fact, we note that

$$T_*(x) = \int_0^{T_*(x)} \frac{\frac{dX}{ds}(-s, x)}{w(X(-s, x))} ds = \int_1^x \frac{dy}{w(y)},$$

which tends to  $+\infty$  as  $x$  tends to  $b$  owing to (7).

We integrate (10) along the characteristics, so that we get

$$\frac{d}{ds} [\ln(f(t+s, X(s, x)))] = -w'(X(s, x)).$$

Finally, we obtain the formula

$$f(t, x) = f_0(X(-t, x)) J(-t, x) \mathbb{1}_{0 \leq t \leq T_*(x)} + \frac{k(t - T_*(x))}{w(1)} J(-T_*(x), x) \mathbb{1}_{t \geq T_*(x)}.$$

For given smooth data  $f_0 \in C^1(\mathbb{R}^+)$ ,  $k \in C^1(\mathbb{R}^+)$ , this formula clearly defines the solution of (10)-(11). In particular, considering data  $f_0$  supported in  $[1, b]$ , the support of the solution remains in  $[1, b]$ . Furthermore, it also makes sense in a more general context allowing discontinuous data or even measure valued solutions, through the dual formulation

$$\begin{aligned} \int_1^b \varphi(x) f(t, dx) &= \int_1^b \varphi(X(t, y)) f_0(dy) \\ &\quad + \int_1^b \varphi(x) \frac{k(t - T_*(x))}{w(1)} J(-T_*(x), x) \mathbb{1}_{t \geq T_*(x)} dx, \end{aligned}$$

which holds for any  $\varphi \in C^1([1, b])$ . The last integral can be rewritten by using the change of variables

$$s = T_*(x), \quad x = X(s, 1), \quad dx = w(X(s, 1)) ds.$$

We end up with

$$\int_1^b \varphi(x) f(t, dx) = \int_1^b \varphi(X(t, y)) f_0(dy) + \int_0^t \frac{k(t-s)}{w(1)} w\varphi(X(s, 1)) J^{-1}(s, 1) ds. \quad (14)$$

**Definition 2.1.** Let  $\mathcal{M}_+^1$  the positive cone of bounded measures on  $[1, b]$ , that is the set of continuous and non negative linear forms on  $C^0([1, b])$ .

For given  $f_0 \in \mathcal{M}_+^1$  and  $k \in L^p(0, T)$  the formula (14) defines the unique solution  $f \in C^0(0, T; \mathcal{M}^1 - \text{weak} - \star)$  of (10)-(11). It means that for any  $\varphi \in C^0([1, b])$ , we have

- there exists  $C_T > 0$  such that for any  $0 \leq t \leq T$ ,  $\left| \int_1^b \varphi(x) f(t, dx) \right| \leq C_T \|\varphi\|_\infty$ ,
- the function  $t \mapsto \int_1^b \varphi(x) f(t, dx)$  is continuous on  $[0, T]$ .

We are thus led to the following definition.

**Definition 2.2.** A measure-valued function  $t \mapsto \rho(t, dx)$  such that

$$\rho \in L^\infty(\mathbb{R}^+; \mathcal{M}_+^1([1, b])) \cap C^0(0, T; \mathcal{M}^1 - \text{weak} - \star)$$

is said a solution of

$$\begin{aligned} \partial_t \rho + \partial_x(w\rho) &= 0, \\ w\rho(t, 1) &= \int_1^b \beta(y) \rho(t, dy), \\ \rho|_{t=0} &= f_0, \end{aligned} \quad (15)$$

if (14) is satisfied for any  $\varphi \in C^0([1, b])$  with  $k(t) = \int_1^b \beta(y) \rho(t, dy) \in C^0(\mathbb{R}^+)$ .

Then, we use a standard fixed point procedure to find the solution of (10)-(11) with the self-consistent boundary condition

$$k(t) = \int_1^b \beta(y) f(t, dy).$$

We set the sequence  $(f^{(n)})_{n \in \mathbb{N}}$  defined by:

$$\begin{aligned} \partial_t f^{(n+1)} + \partial_x(wf^{(n+1)}) &= 0, \\ wf^{(n+1)}(t, 1) &= \int_1^b \beta(y) f^{(n)}(t, dy), \\ f^{(n+1)}|_{t=0} &= f_0, \end{aligned}$$

and as initial guess we choose

$$f^{(0)} \equiv 0.$$

We show that the sequence is non-decreasing and bounded. By induction the sequence  $(f^{(n)})_{n \in \mathbb{N}}$  is non-decreasing; in fact, for any  $\varphi \in C^1([1, b])$ ,  $\varphi \geq 0$ ,

$$\int_1^b \varphi(x) (f^{(1)} - f^{(0)})(t, dx) = \int_1^b \varphi(X(t, y)) f_0(dy) \geq 0,$$

and

$$\begin{aligned} & \int_1^b \varphi(x) (f^{(n+1)} - f^{(n)})(t, dx) \\ &= \int_0^t ds \left( \int_1^b \beta(y) (f^{(n)} - f^{(n-1)})(t-s, dy) \right) w\varphi(X(s, 1)) \frac{J^{-1}(s, 1)}{w(1)}. \end{aligned}$$

So we deduce that  $f^{(n+1)} - f^{(n)} \geq 0$  for any  $n \in \mathbb{N}$ .

We prove the boundeness also by induction; assume that

$$\forall \varphi \in C^1([1, b]), \|\varphi\|_\infty \leq 1, \sup_{0 \leq t < \infty} \left| \int_1^b \varphi(y) e^{-\mu t} f^{(n)}(t, dy) \right| \leq M,$$

where  $\mu > 0$  and  $M > 0$  will be set further on. Then, we have for any test function  $\varphi$  with  $\|\varphi\|_\infty \leq 1$ ,

$$\begin{aligned} & \left| \int_1^b \varphi(x) f^{(n+1)}(t, dx) e^{-\mu t} \right| \\ & \leq \int_1^b |f_0(dy)| e^{-\mu t} \\ & \quad + \left| \int_0^t ds \left( \int_1^b \beta(y) e^{-\mu(t-s)} f^{(n)}(t-s, dy) \right) w\varphi(X(s, 1)) \frac{J^{-1}(s, 1)}{w(1)} e^{-\mu s} \right| \\ & \leq \int_1^b |f_0(dy)| e^{-\mu t} + \int_0^t \|\beta\|_\infty M \frac{\|w\|_\infty}{w(1)} J^{-1}(s, 1) e^{-\mu s} ds. \end{aligned} \quad (16)$$

Since, according to (5)

$$0 \leq J^{-1}(s, 0) = \exp \left( \int_s^0 w'(X(\sigma, x)) d\sigma \right) \leq \exp(sL),$$

we have:

$$\left| \int_1^b \varphi(x) f^{(n+1)}(t, dx) e^{-\mu t} \right| \leq \int_1^b |f_0(dy)| e^{-\mu t} + \frac{\|\beta\|_\infty \|w\|_\infty}{w(1)} \frac{M}{\mu - L}.$$

We choose  $\mu$  and  $M$  such that

$$\alpha := \frac{\|\beta\|_\infty \|w\|_\infty}{w(1)(\mu - L)} < 1 \quad \text{and} \quad \frac{\int_1^b |f_0(dy)|}{1 - \alpha} \leq M.$$

Then

$$\sup_{0 \leq t < \infty} \left| \int_1^b \varphi(x) f^{(n+1)}(t, dx) e^{-\mu t} \right| \leq M,$$

holds for any  $\varphi \in C^1([1, b])$  verifying  $\|\varphi\|_\infty \leq 1$ . Therefore, for any  $n \in \mathbb{N}$ , we deduce that

$$\sup_{0 \leq t < \infty} e^{-\mu t} \|f^{(n)}(t)\|_{\mathcal{M}^1} \leq M.$$

We end the proof by establishing a contraction property. We fix  $\varphi = \beta$ , and we get

$$\begin{aligned} & 0 \leq \int_1^b \beta(x) (f^{(n+1)} - f^{(n)})(t, dx) e^{-\mu t} \\ & = \int_0^t ds \left( \int_1^b \beta(x) e^{-\mu(t-s)} (f^{(n)} - f^{(n-1)})(t-s, dy) \right) w\beta(X(s, 1)) e^{-\mu s} \frac{J^{-1}(s, 1)}{w(1)} \\ & \leq \sup_{\tau \geq 0} \left( e^{-\mu\tau} \int_1^b \beta(y) (f^{(n)} - f^{(n-1)})(\tau, dy) \right) \int_0^t w\beta(X(s, 1)) e^{-\mu s} \frac{J^{-1}(s, 1)}{w(1)} ds \\ & \leq \sup_{\tau \geq 0} \left( e^{-\mu\tau} \int_1^b \beta(y) (f^{(n)} - f^{(n-1)})(\tau, dy) \right) \frac{\|w\|_\infty \|\beta\|_\infty}{w(1)(\mu - L)} \\ & \leq \alpha \sup_{\tau \geq 0} \left( e^{-\mu\tau} \int_1^b \beta(y) (f^{(n)} - f^{(n-1)})(\tau, dy) \right), \end{aligned}$$

where, by definition,  $0 < \alpha < 1$ . Hence, the sequence  $(f^{(n)})_{n \in \mathbb{N}}$  converges and the limit fulfills the requirements of Definition 2.2.

**Theorem 2.3.** *Assume (5)-(6). Let  $f_0 \in \mathcal{M}_+^1$ . Then, there exists a unique solution of (15) in the sense of Definition 2.2.*

**Remark 1.** The proof also shows that if the initial data is absolutely continuous with respect to the Lebesgue measure, then the solution is absolutely continuous with respect to the Lebesgue measure too.

At first look, this statement does not fit the resolution of the original system (1)-(4). However, we note that  $\delta(x = X(t, 0))$  satisfies (14) with  $f_0 = \delta(x = 1)$  and  $k = 0$ . Accordingly we show that  $\rho$  satisfies (10)-(11) with  $k(t) = \int_1^b \beta \rho(t, dx) + \beta(X(t, 0))$  and  $f_0 = 0$  iff  $f = \rho + \delta(x = X(t, 0))$  satisfies (10)-(11) with  $k(t) = \int_1^b \beta \rho(t, dx)$  and  $f_0 = \delta(x = 1)$ . This remark shows that (1)-(4) is equivalent to (15) with initial data  $\delta(x = 1)$ . Note however that the interpretation is slightly changed since  $\rho$  represents secondary tumors only, while  $f$  represents the primary and secondary tumors.

**Corollary 1.** *Assume (5)-(6). Then, there exists a unique solution in the set  $L^\infty(\mathbb{R}^+; \mathcal{M}_+^1([1, b])) \cap C^0(\mathbb{R}^+; \mathcal{M}_+^1 - \text{weak} - \star)$  to (1)-(4).*

**2.2. A generational point of view.** The total population of metastasis is composed of the daughters, the granddaughters, the great-granddaughters, etc. of the primary tumor, hence the total population of metastasis can be structured by the rank in the line of descent from the primary tumor and the total density of population can be seen as the sum of the density of each of these sub-populations. Let us denote by  $\rho_n$  the density of the population of rank  $n$  in the line of descent. Then  $\rho_1$  will denote the population of the daughter-metastasis of the primary tumor. We have the following recursion:

$$\partial_t \rho_{n+1} + \partial_x (w \rho_{n+1}) = 0, \tag{17a}$$

$$\rho_{n+1}|_{t=0} = 0, \tag{17b}$$

$$w(1) \rho_{n+1}(t, 1) = \int_1^b \beta(x) \rho_n(t, x) dx, \tag{17c}$$

with the initialization:

$$\partial_t \rho_1 + \partial_x (w \rho_1) = 0,$$

$$\rho_1|_{t=0} = 0,$$

$$w(1) \rho_1(t, 1) = \beta(x_p(t)),$$

where  $x_p$  is defined in (3). We set then

$$\rho = \sum_{n=1}^{\infty} \rho_n. \tag{18}$$

A proof very similar to the previous one, justifies the convergence of the series and shows that  $\rho$  defined in (18) is solution of (1)-(4). We refer to the fifth section for numerical simulations and a discussion on the contribution of each generation in the total population density.

**3. Eigenproblem.** In this section we are concerned with the eigenproblem associated to (15). We aim at establishing the existence of a unique positive eigenvalue associated to a positive eigenvector and dual eigenvector, namely we seek  $(\lambda_0, N, \Phi)$  satisfying

$$\frac{\partial}{\partial x} (N(x)w(x)) + \lambda_0 N(x) = 0, \quad (19a)$$

$$w(1)N(1) = \int_1^b \beta(y)N(y) dy, \quad (19b)$$

$$-w(x)\frac{\partial}{\partial x}\Phi(x) + \lambda_0\Phi(x) = \Phi(1)\beta(x), \quad (19c)$$

$$\lambda_0 > 0, \quad N \geq 0, \quad \Phi \geq 0, \quad \int_1^b N\Phi dx = 1, \quad \int_1^b N dx = 1. \quad (19d)$$

**Theorem 3.1.** *There exists a unique  $\lambda_0 > 0$  and  $(N, \Phi) \in L^1([1, b]) \times L^\infty([1, b])$  satisfying (19a)-(19d).*

*Proof.* We start by studying (19a)-(19b). We set the change of variable:  $x = x_p(t)$ , where  $x_p$  is defined by (3), and we define

$$U(t) = (wN)(x_p(t)).$$

Then (19a)-(19b) recasts as

$$\begin{cases} \partial_t U + \lambda_0 U = 0, \\ U(0) = \int_0^\infty B(t)U(t) dt, \end{cases} \quad (20)$$

where  $B(t) = \beta(x_p(t))$ . This mere ODE can be integrated and we get

$$U(t) = e^{-\lambda_0 t} \int_0^\infty B(s)U(s) ds. \quad (21)$$

We have  $\int_0^\infty BU ds \neq 0$ : indeed if  $\int_0^\infty BU ds = 0$ , then, due to the non degeneracy condition (6),  $U \equiv 0$  and  $U$  can not be a eigenvector. We multiply (21) by  $B$  and integrate:

$$\int_0^\infty B(t)U(t) dt = \int_0^\infty B(t)e^{-\lambda_0 t} dt \cdot \int_0^\infty B(s)U(s) ds.$$

Since  $\int_0^\infty BU ds \neq 0$ , we deduce that

$$\int_0^\infty B(t)e^{-\lambda_0 t} dt = 1.$$

We set

$$F(\mu) := \int_0^\infty B(t)e^{-\mu t} dt.$$

Clearly,  $F$  is decreasing and we note that  $F(\infty) = 0$  since  $B$  is bounded, and

$$F(0) = \int_0^\infty B(t) dt = \int_1^b \frac{\beta(x)}{w(x)} dx = +\infty,$$

(see (7)). We conclude that

$$\exists! \lambda_0 \in (, \infty) \text{ s.t. } F(\lambda_0) = 1, \quad (22)$$

and, according to (21),  $U(t) = U(0)e^{-\lambda_0 t}$  is a solution of (20) associated to the eigenvalue  $\lambda_0$ .

Next, we check that the eigenspace associated to  $\lambda_0$  is of dimension one. Let  $v(t)$  be another eigenvector associated to  $\lambda_0$ . Since we can write

$$v(t) = CU(t) + \bar{v}(t),$$

where  $\bar{v}$  is such that  $\int_0^\infty \bar{v}(t)U(t) dt = 0$ , we can assume that  $\int_0^\infty e^{-\lambda_0 s} v(s) ds = 0$ . Moreover, we seek  $v$  in  $W^{1,1}(\mathbb{R}^+)$  and assume  $v \neq 0$ . Then, we have

$$\begin{aligned} \int_0^\infty v'(s) ds &= -v(0) \\ &= \left[ e^{-\lambda_0 t} v(t) \right]_0^\infty = \int_0^\infty (-\lambda_0 e^{-\lambda_0 t} v(t) + e^{-\lambda_0 t} v'(t)) dt \\ &= -2\lambda_0 \int_0^\infty e^{-\lambda_0 t} v(t) dt = 0. \end{aligned}$$

However, (20) implies that

$$\int_0^\infty v'(s) ds = -v(0) = -\int_0^\infty B(s)v(s) ds,$$

which yields a contradiction since  $\int_0^\infty B(s)v(s) ds \neq 0$  otherwise  $v$  would be identically 0 by (21). We conclude that the eigenspace associated to  $\lambda_0$  is  $\text{Span}\{t \mapsto e^{-\lambda_0 t}\}$ . Coming back to the original variables yields

$$N(x) = \frac{U(0)}{a \ln b} \frac{1}{x} \left( 1 - \frac{\ln x}{\ln b} \right)^{\lambda_0/a-1}, \quad (23)$$

which is integrable since  $\frac{\lambda_0}{a} - 1 > -1$  (but the behavior for  $x$  next to  $b$  depends on the sign of  $\frac{\lambda_0}{a} - 1$ ).

Turning now to the dual problem (19c), we set again the change of variable  $x = x_p(t)$ , and we get for  $\Psi(t) = \Phi(x_p(t))$ ,

$$-\frac{\partial \Psi}{\partial t} + \lambda_0 \Psi = \Psi(0)B(t),$$

where  $\lambda$  is defined by (22), which means that:

$$\Psi(t) = e^{\lambda_0 t} \Psi(0) \left[ 1 - \int_0^t B(u)e^{-\lambda_0 u} du \right].$$

Since, according to (22),  $\int_0^\infty B(u)e^{-\lambda_0 u} du = 1$  and  $B(u)e^{-\lambda_0 u} > 0$ , we have  $\Psi > 0$  when  $\Psi(0) > 0$ . Moreover, we have

$$\Psi(t) = \Psi(0) \int_t^\infty B(u)e^{-\lambda_0(u-t)} du \leq \frac{\Psi(0)\|\beta\|_\infty}{\lambda_0}.$$

This shows that  $\Psi$  is bounded, so  $\Phi \in L^\infty([1, b])$ . To satisfy the normalization conditions, we choose convenient constants  $U(0)$  and  $\Psi(0)$ .  $\square$

**4. General relative entropy and asymptotic behavior.** The general relative entropy method is currently used for McKendrick-Von Foerster equations (see [11]) to find *a priori* bounds and to describe the asymptotic behavior of the solution. It is based on the eigenproblem described before.

#### 4.1. Conservation law and general relative entropy.

**Theorem 4.1.** *Let  $(N, \lambda_0, \Phi)$  be a solution of the problem (19a)-(19d), then for any  $\rho(0, \cdot) \geq 0$  and any  $\rho(t, \cdot)$  solution of (15) with initial data  $\rho(0, \cdot) \in L^\infty([1, b], \frac{dx}{N})$ ,*

1. *we have the conservation law*

$$\int_1^b \Phi(x) \rho(t, x) e^{-\lambda_0 t} dx = \int_1^b \Phi(x) \rho(0, x) dx, \quad (24)$$

2. *for any convex function  $H$ , the general relative entropy defined as*

$$\frac{d}{dt} \int_1^b \Phi(x) N(x) H \left( \frac{\rho(t, x) e^{-\lambda_0 t}}{N(x)} \right) dx := -D_H, \quad (25)$$

with

$$\begin{aligned} -D_H &= w(1)N(1)\Phi(1) \\ &\times \left[ H \left( \int_1^b \frac{\rho(t, x) e^{-\lambda_0 t}}{N(x)} d\mu(x) \right) - \int_1^b H \left( \frac{\rho(t, x) e^{-\lambda_0 t}}{N(x)} \right) d\mu(x) \right], \end{aligned} \quad (26)$$

where

$$d\mu(x) = \frac{\beta(x)N(x)}{w(1)N(1)} dx,$$

is non positive.

*Proof.* Remark first that the conservation law can be obtained from the entropy formula, by choosing  $H(x) = x$ , since  $-D_H$  is zero in this case. In order to obtain (25) we develop its left hand side:

$$\begin{aligned} -D_H &= \frac{d}{dt} \int_1^b \Phi(x) N(x) H \left( \frac{\rho(t, x) e^{-\lambda_0 t}}{N(x)} \right) dx, \\ &= \int_1^b \Phi N \left[ \partial_t \rho \frac{e^{-\lambda_0 t}}{N} - \lambda N \frac{\rho e^{-\lambda_0 t}}{N^2} \right] H' \left( \frac{\rho e^{-\lambda_0 t}}{N} \right) dx, \\ &= \int_1^b \Phi N \left[ -\partial_x (w\rho) \frac{e^{-\lambda_0 t}}{N} + \partial_x (wN) \frac{\rho e^{-\lambda_0 t}}{N^2} \right] H' \left( \frac{\rho e^{-\lambda_0 t}}{N} \right) dx, \\ &= \int_1^b \Phi N \left[ -w(\partial_x \rho) \frac{e^{-\lambda_0 t}}{N} + (\partial_x N) w \frac{\rho e^{-\lambda_0 t}}{N^2} \right] H' \left( \frac{\rho e^{-\lambda_0 t}}{N} \right) dx, \\ &= - \int_1^b \Phi N w \partial_x \left( \frac{\rho e^{-\lambda_0 t}}{N} \right) H' \left( \frac{\rho e^{-\lambda_0 t}}{N} \right) dx, \\ &= w(1)\Phi(1)N(1)H \left( \frac{\rho(t, 1) e^{-\lambda_0 t}}{N(1)} \right) - \int_1^b \Phi(1)\beta N H \left( \frac{\rho e^{-\lambda_0 t}}{N} \right) dx, \\ &= w(1)N(1)\Phi(1) \left[ H \left( \int_1^b \frac{\rho(t, x) e^{-\lambda_0 t}}{N(x)} d\mu(x) \right) \right. \\ &\quad \left. - \int_1^b H \left( \frac{\rho(t, x) e^{-\lambda_0 t}}{N(x)} \right) d\mu(x) \right]. \end{aligned}$$

Therefore  $D_H$  is non negative by virtue of the Jensen Lemma since  $H$  is convex and  $d\mu$  is a probability measure.  $\square$

**Proposition 1.** For  $H(x) = x^2$ ,  $D_H$  vanishes iff  $\frac{\rho(t, \cdot)e^{-\lambda_0 t}}{N(\cdot)} = C(t)$  does not depend on  $x$ .

*Proof.* It is a consequence of the equality case in the Cauchy–Schwarz inequality.  $\square$

**4.2. Boundedness properties.** We deduce from the fact that entropy is decreasing some *a priori* bounds, according to [12], [11]. In fact, by using Theorem 4.1, we get:

- **$L^\infty$  bound.:** Let  $C \geq 0$ . Then, choosing  $H(x) = (x - C)^+$  which is convex non negative, we get

$$\rho(0, \cdot) \leq CN(\cdot) \implies \forall t \geq 0, \quad \rho(t, \cdot)e^{-\lambda_0 t} \leq CN(\cdot). \quad (27)$$

- **$L^\infty$  bound.:** Let  $c \geq 0$ . Choosing  $H(x) = (c - x)^+$  which is convex non negative, we get in the same way

$$\rho(0, \cdot) \geq cN(\cdot) \implies \forall t \geq 0, \quad \rho(t, \cdot)e^{-\lambda_0 t} \geq cN(\cdot). \quad (28)$$

- **$L^p$  bound.:** Choosing  $H(x) = |x|^p$  which is convex non negative, we finally get

$$\frac{\rho(0, \cdot)}{N(\cdot)} \in L^p([0, b], N\Phi \, dx) \implies \forall t \geq 0, \quad \frac{\rho(t, \cdot)e^{-\lambda_0 t}}{N(\cdot)} \in L^p([0, b], N\Phi \, dx) \quad (29)$$

and

$$\forall t \geq 0, \quad \int_1^b \left( \frac{\rho(t, x)e^{-\lambda_0 t}}{N(x)} \right)^p N(x)\Phi(x) \, dx \leq \int_1^b \left( \frac{\rho(0, x)}{N(x)} \right)^p N(x)\Phi(x) \, dx.$$

**4.3. Asymptotic behavior.** In this Section, we investigate the large time asymptotics. We describe first the asymptotic behaviour and then we detail the convergence rate to the asymptotic.

**4.3.1. Long time asymptotic.**

**Theorem 4.2.** For any  $\rho(0, \cdot) \geq 0$  such that  $\frac{\rho(0, \cdot)}{N(\cdot)} \in L^\infty \cap L^2([0, b], N\Phi \, dx)$  and any  $\rho(t, \cdot)$  solution of (15) with initial data  $\rho(0, \cdot)$  then the following convergence

$$\frac{\rho(\cdot, t)e^{-\lambda_0 t}}{N(\cdot)} \xrightarrow[t \rightarrow \infty]{} \int_1^b \Phi(x)\rho(0, x) \, dx, \quad (30)$$

holds in  $L^\infty \cap L^2([0, b], N\Phi \, dx)$  as  $t$  tends to  $\infty$ .

The proof is based on the entropy dissipation, still following the approach of [12]; for a similar result obtained by using semi-group techniques, we refer to [2].

**Notation.** In this section, given  $T \geq 0$ , we will use the following notations:

$$\begin{aligned} -D_{H,T}(t) &= \int_1^b H \left( \frac{\rho(t+T, x)e^{-\lambda_0(t+T)}}{N(x)} \right) d\mu(x) \\ &\quad - H \left( \int_1^b \frac{\rho(t+T, x)e^{-\lambda_0(t+T)}}{N(x)} d\mu(x) \right) \end{aligned}$$

and

$$v_T(t, x) = \rho(t+T, x)e^{-\lambda_0(t+T)}.$$

We start by proving the following lemma:

**Lemma 4.3.** *For any convex function  $H$ , we have*

$$\forall t \geq 0, \quad \lim_{T \rightarrow \infty} \int_0^t D_{H,T}(s) \, ds = 0. \quad (31)$$

*Proof.* Writing (25)-(26) at time  $t = s + T$  yields for any  $T \geq 0$

$$\frac{d}{ds} \int_1^b \Phi(x) N(x) H \left( \frac{\rho(s+T, x) e^{-\lambda_0(s+T)}}{N(x)} \right) dx + w(1) \Phi(1) N(1) D_{H,T}(s) = 0.$$

By integration over  $s \in (0, t)$ , we get:

$$\begin{aligned} & \int_1^b \Phi(x) N(x) H \left( \frac{\rho(t+T, x) e^{-\lambda_0(t+T)}}{N(x)} \right) dx + w(1) \Phi(1) N(1) \int_0^t D_{H,T}(s) \, ds \\ &= \int_1^b \Phi(x) N(x) H \left( \frac{\rho(T, x) e^{-\lambda_0 T}}{N(x)} \right) dx. \end{aligned} \quad (32)$$

Since

$$t \mapsto \int_1^b \Phi(x) N(x) H \left( \frac{\rho(t, x) e^{-\lambda_0 t}}{N(x)} \right) dx$$

is non increasing and positive, it has a limit as  $t$  tends to infinity. Passing to the limit  $T \rightarrow \infty$  in (32), we get (31).  $\square$

In what follows, we fix  $H(x) = x^2$ . According to Lemma 4.3, we have:

$$\lim_{T \rightarrow \infty} \int_0^t \left[ \int_1^b \left( \frac{v_T(s, x)}{N} \right)^2 d\mu(x) - \left( \int_1^b \frac{v_T(s, x)}{N} d\mu(x) \right)^2 \right] ds = 0. \quad (33)$$

Next, we shall investigate the passage to the limit in both integrals arising in (33).

**Lemma 4.4.** *Assume that  $\frac{\rho(0, \cdot)}{N(\cdot)} \in L^2([0, b], N\Phi \, dx)$  then for any  $t \geq 0$  it exists a sequence  $(T_n)_n \rightarrow \infty$  and  $v \in L^\infty([0, t], L^2([1, b], \frac{\Phi}{N}))$  such that*

$$\liminf_{T_n \rightarrow \infty} \int_0^t \int_1^b \left( \frac{v_{T_n}(s, x)}{N(x)} \right)^2 d\mu(x) \, ds \geq \int_0^t \int_1^b \left( \frac{v(s, x)}{N(x)} \right)^2 d\mu(x) \, ds.$$

*Proof.* According to (29),  $\left( v_T(s, \cdot) \sqrt{\frac{\Phi(\cdot)}{N(\cdot)}} \right)$  is bounded in  $L^2((0, t) \times (1, b))$ , uniformly with respect to  $T \geq 0$ . Therefore, by the Banach-Alaoglu theorem, there exists a sequence  $(T_n)_n$  and  $v \in L^2\left((0, t) \times (1, b), \frac{\Phi(\cdot)}{N(\cdot)} \, dx \, ds\right)$  such that

$$v_{T_n} \sqrt{\frac{\Phi}{N}} \rightharpoonup v \sqrt{\frac{\Phi}{N}},$$

where the convergence holds weakly in  $L^2((0, T) \times (1, b))$ . Moreover, we have

$$\begin{aligned} \int_0^t \int_1^b v_{T_n}^2(s, x) \frac{\beta(x)}{N(x)} \, dx \, ds &= \int_0^t \int_1^b \left( v_{T_n}(s, x) \sqrt{\frac{\Phi(x)}{N(x)}} \right)^2 \frac{\beta(x)}{\Phi(x)} \, dx \, ds, \\ &\geq \int_0^t \int_1^b \left( v_{T_n}(s, x) \sqrt{\frac{\Phi(x)}{N(x)}} \right)^2 \Psi_\eta(x) \, dx \, ds, \end{aligned}$$

where we denote by  $\Psi_\eta$  the function

$$\Psi_\eta(x) := \frac{\beta(x)}{\Phi(x)} \mathbb{1}_{x \leq b-\eta}.$$

By convexity, for any  $\varphi \in L^\infty([1, b])$ ,  $\varphi \geq 0$ , we have

$$\begin{aligned} & \liminf_{n \rightarrow \infty} \int_0^t \int_1^b \left( v_{T_n}(s, x) \sqrt{\frac{\Phi(x)}{N(x)}} \right)^2 \varphi(x) \, dx \, ds \\ & \geq \int_0^t \int_1^b \left( v(s, x) \sqrt{\frac{\Phi(x)}{N(x)}} \right)^2 \varphi(x) \, dx \, ds. \end{aligned}$$

In particular it holds for  $\varphi = \Psi_\eta$  so that

$$\liminf_{n \rightarrow \infty} \int_0^t \int_1^b v_{T_n}^2(s, x) \frac{\beta(x)}{N(x)} \, dx \, ds \geq \int_0^t \int_1^b \left( v(s, x) \sqrt{\frac{\Phi(x)}{N(x)}} \right)^2 \Psi_\eta(x) \, dx \, ds,$$

We pass to the limit in the right hand side, using the monotone convergence theorem as  $\eta$  tends to 0. We get

$$\liminf_{n \rightarrow \infty} \int_0^t \int_1^b v_{T_n}^2(s, x) \frac{\beta(x)}{N(x)} \, dx \, ds \geq \int_0^t \int_1^b \left( \frac{v(s, x)}{N(x)} \right)^2 N(x) \beta(x) \, dx \, ds,$$

which proves the lemma.  $\square$

**Lemma 4.5.** *Assume that there exists a constant  $C \geq 0$ , such that  $\rho(0, \cdot) \leq CN(\cdot)$ , then for any  $t \geq 0$  there exists a sequence  $(T_n)_n \rightarrow \infty$  and  $v \in \mathcal{C}^0([0, t], \mathcal{M}^1([1, b]) - \text{weak} - *)$  such that*

$$\int_1^b \frac{v_{T_n}(s, x)}{N(x)} \, d\mu(x) \longrightarrow \int_1^b \frac{v(s, x)}{N(x)} \, d\mu(x),$$

uniformly on  $[0, t]$  as  $(T_n)_n$  tends to  $\infty$ .

*Proof.* For any  $\varphi \in \mathcal{C}^1([1, b])$ , we set

$$V_T^{[\varphi]}(s) = \int_1^b v_T(s, x) \varphi(x) \, dx.$$

Clearly, we have

$$\left| V_T^{[\varphi]}(s) \right| \leq C \|\varphi\|_\infty, \quad (34)$$

owing to (27). Next, we compute

$$\begin{aligned} \frac{d}{ds} V_T^{[\varphi]}(s) &= \int_1^b \left[ \partial_s (\rho(s+T, x)) e^{-\lambda_0(s+T)} \varphi(x) - \lambda_0 \rho(s+T, x) e^{-\lambda_0(s+T)} \varphi(x) \right] \, dx, \\ &= \int_1^b w(x) \rho(s+T, x) e^{-\lambda_0(s+T)} \varphi'(x) \, dx + w(1) \varphi(1) \rho(s+T, 1) e^{-\lambda_0(s+T)} \\ &\quad - \lambda_0 \int_1^b \rho(s+T, x) e^{-\lambda_0(s+T)} \varphi(x) \, dx, \\ &= \int_1^b [w(x) \varphi'(x) - \lambda_0 \varphi(x) + \varphi(1) \beta(x)] v_T(s, x) \, dx. \end{aligned}$$

Since  $\|w\|_\infty = ab/e$ , by using (27) again, we get,

$$\forall \varphi \in \mathcal{C}^1([1, b]), \quad \left| \frac{d}{ds} V_T^{[\varphi]}(s) \right| \leq C \|\varphi\|_{W^{1,\infty}},$$

which proves that  $\left( s \mapsto V_T^{[\varphi]}(s) \right)_{T \geq 0}$  is equicontinuous on  $[0, t]$  for any  $t > 0$ . Therefore, by the Arzela–Ascoli theorem, for any  $\varphi \in \mathcal{C}^1([1, b])$  it belongs to a compact set of  $\mathcal{C}^0([0, t])$ . By (34) and a density argument, this is also true for any  $\varphi \in \mathcal{C}^0([1, b])$ . Then using both separability and the diagonal Cantor process, we can find a subsequence  $T_n$ , and  $v \in \mathcal{C}^0([0, \infty), \mathcal{M}^1([1, b] - weak - *))$  such that the following convergence

$$V_{T_n}^{[\varphi]}(s) \longrightarrow \int_1^b v(s, x) \varphi(x) dx,$$

as  $(T_n)$  tends to infinity, holds uniformly on  $[0, t]$ , for any  $\varphi \in \mathcal{C}^0([1, b])$  and any  $t \geq 0$ . Then we fix  $\varphi = \beta/(N(1)w(1))$  and it proves the lemma.  $\square$

Note that we can identify the limit  $v$  arising in Lemma 4.4 and 4.5 and Lemma 4.5 allows to pass to the limit in the second term in (33). Now, we go back to (33); using Lemma 4.4 and 4.5, we obtain

$$\begin{aligned} 0 &= \lim_{T_n \rightarrow \infty} \int_0^t \left[ \int_1^b \left( \frac{v_{T_n}(s, x)}{N} \right)^2 d\mu(x) - \left( \int_1^b \frac{v_{T_n}(s, x)}{N} d\mu(x) \right)^2 \right] ds, \\ &\geq \liminf_{T_n \rightarrow \infty} \int_0^t \int_1^b \left( \frac{v_{T_n}(s, x)}{N} \right)^2 d\mu(x) ds - \lim_{T_n \rightarrow \infty} \int_0^t \left( \int_1^b \frac{v_{T_n}(s, x)}{N} d\mu(x) \right)^2 ds, \\ &\geq \int_0^t \int_1^b \left( \frac{v(s, x)}{N} \right)^2 d\mu(x) ds - \int_0^t \left( \int_1^b \frac{v(s, x)}{N} d\mu(x) \right)^2 ds \geq 0. \end{aligned}$$

We conclude by using Proposition 1 to obtain that the following convergence

$$\frac{\rho(\cdot, t)e^{-\lambda_0 t}}{N(\cdot)} \rightarrow C, \tag{35}$$

holds in  $L^\infty \cap L^2([0, b], N\Phi dx)$  as  $t$  tends to infinity. The constant is indeed uniquely determined by using the conservation law (24) and the normalization condition imposed on the eigenvectors (19d). In fact Proposition 1 shows that

$$\frac{v(s, \cdot)}{N(\cdot)} = C(s).$$

But (24) gives us

$$\int_1^b v_{T_n}(s, x) \Phi(x) dx = \int_1^b \rho(0, x) \Phi(x) dx,$$

and using arguments similar to the ones detailed in the proof of Lemma 4.5, we can pass to the limit and get

$$\int_1^b v(s, x) \Phi(x) dx = \int_1^b \rho(0, x) \Phi(x) dx,$$

which, using (19d), leads us to

$$\int_1^b N(x) \Phi(x) C(s) dx = C(s) = \int_1^b \rho(0, x) \Phi(x) dx.$$

Then  $C(s)$  does not depend on  $s$  and is uniquely defined. We conclude that the whole sequence converge with

$$C = \int_1^b \Phi(x)\rho(0, x) dx. \quad (36)$$

This completes the proof of Theorem 4.2.

4.3.2. *Convergence rate.* We are now interested in the rate of convergence of (30). The method we use is based on the invariant (24) and is inspired from [6].

In order to state our convergence result we need to rewrite the equation after renormalization by the exponential growth of the system. We define

$$\tilde{\rho}(t, x) = \rho(t, x)e^{-\lambda_0 t}.$$

Then,  $\tilde{\rho}(t, x)$  satisfies the equations

$$\begin{cases} \partial_t \tilde{\rho}(t, x) + \partial_x(w(x)\tilde{\rho}(t, x)) + \lambda_0 \tilde{\rho}(t, x) = 0, \\ w(1)\tilde{\rho}(t, 0) = \int_1^b \beta(y)\tilde{\rho}(t, y) dy, \end{cases}$$

with initial condition  $\tilde{\rho}(t = 0, x) = \tilde{\rho}^0(x) \in L^1([1, b])$ . As a consequence of the general relative entropy principle we have the conservation law (see (24))

$$\frac{d}{dt} \int_1^b \tilde{\rho}(t, x)\Phi(x) = 0. \quad (37)$$

Finally, we introduce the function

$$h(t, x) = \tilde{\rho}(t, x) - \left( \int_1^b \rho^0(y)\Phi(y) dy \right) N(x).$$

Then  $h(t, x)$  fulfills

$$\begin{cases} \partial_t h(t, x) + \partial_x(w(x)h(t, x)) + \lambda_0 h = 0, \\ w(1)h(1) = \int_1^b \beta(x)h(t, x) dx, \end{cases} \quad (38)$$

with initial condition  $h(t = 0, x) = h^0(x)$ .

Note that the conservation law (37) implies that

$$\forall t \geq 0, \int_1^b h(t, x)\Phi(x) dx = 0. \quad (39)$$

In what follows  $X(t, x)$  designed the characteristic defined at (12) and  $J(-t, x)$  is the jacobian of the change of variable  $y = X(-t, x)$  (see (13)). The key assumption reads :

**Assumption 1.** The following property holds

$\exists \mu_0 > 0$ , and  $y \in [0, \infty)$ , such that,  $\forall u \in [1, b]$ ,  $u \geq X(y, 1)$ , we have

$$\Phi(1)\beta(u)N(u) \geq \mu_0 N(X(-y, u))\Phi(X(-y, u))J(-y, u). \quad (40)$$

We have the following result concerning the convergence rate. It is exponential.

**Theorem 4.6.** *The solutions to (38) satisfy*

$$\int_{X(y,1)}^b \frac{h(t,u)}{N(u)} N(X(-y,u)) \Phi(X(-y,u)) J(-y,u) du = 0, \quad \forall t \geq y \geq 0. \quad (41)$$

Additionally, assume that Assumption. 1 holds, then

$$\int_1^b |h(t,x)| \Phi(x) dx \leq \min \left\{ 1, e^{-\mu_0(t-y)} \right\} \int_1^b |h^0(x)| \Phi(x) dx.$$

**Remark 2.** In our case it is easy to check that Assumption. 1 is fulfilled with  $y = 0$  and  $\mu_0 = m$ , but this choice can be improved choosing  $y \neq 0$ . In fact one can note that after the change of variable  $x = x_p(t)$  already used at Section. 3, the condition (40) is equivalent to

$$e^{-\lambda_0(t+y)} B(t+y) \geq \mu_0 \int_t^\infty e^{-\lambda_0 u} B(u) du \quad (42)$$

where  $B(t) = \beta(x_p(t))$ . We set:

$$Y : t \in [0, \infty) \mapsto \int_t^\infty e^{-\lambda_0 u} B(u) du$$

and

$$f : t \in [0, \infty) \mapsto \frac{-Y'(t+y)}{Y(t)}.$$

A short analysis shows that  $Y''(t)$  is negative for  $0 \leq t < t_0$  and positive if  $t > t_0$ , where

$$t_0 = \frac{1}{a} \ln \left( \frac{a\alpha \ln b}{\lambda_0} \right).$$

For  $y \geq t_0$ ,  $f$  is then a non-decreasing function and for all  $t \geq 0$ ,  $f(t) \geq f(0) = -Y'(y)$ . Thus, we can choose  $\mu_0 = -Y'(y)$  which is maximal for  $y = t_0$  ( $-Y'(t_0) > m$ ).

*Proof.* The proof is an adaptation of the one proposed in [6], taking into account the characteristics due to the non constant speed rate  $w$ .

**1st step.:** In exactly the same way as in [6], we show that

$$\frac{d}{dt} \int_1^b |h(t,x)| \Phi(x) dx = \Phi(1) \left( \left| \int_1^b \beta(x) h(t,x) dx \right| - \int_1^b \beta(x) |h(t,x)| dx \right), \quad (43)$$

which provides the property:

$$t \mapsto \int_1^b |h(t,x)| \Phi(x) dx \quad \text{is monotone nonincreasing.} \quad (44)$$

**2nd step.:** We have

$$\frac{\partial h(t,x)}{\partial t} \frac{1}{N(x)} + w(x) \frac{\partial h(t,x)}{\partial x} \frac{1}{N(x)} = 0,$$

therefore we also have

$$\frac{h(t-y,x)}{N(x)} = \frac{h(t, X(y,x))}{N(X(y,x))}, \quad \text{for } t \geq y.$$

Thus, using (39), we get:

$$\begin{aligned}
0 &= \int_1^b \frac{h(t-y, x)}{N(x)} \Phi(x) N(x) dx \\
&= \int_1^b \frac{h(t, X(y, x))}{N(X(y, x))} N(x) \Phi(x) dx \\
&= \int_{X(y,1)}^b \frac{h(t, u)}{N(u)} N(X(-y, u)) \Phi(X(-y, u)) J(-y, u) du, \quad \forall t \geq y,
\end{aligned}$$

and (41) is proved.

**3rd step.:** Using (41) and Assumption. 1, for all  $t \geq y$ , it holds

$$\begin{aligned}
&\left| \int_1^b \Phi(1) \beta(x) h(t, x) dx \right| \\
&= \left| \int_1^b \Phi(1) \beta(x) h(t, x) ds \right. \\
&\quad \left. - \mu_0 \int_{X(y,1)}^b \frac{h(t, u)}{N(u)} N(X(-y, u)) \Phi(X(-y, u)) J(-y, u) du \right| \\
&\leq \int_1^b [\Phi(1) \beta(u) N(u) \\
&\quad - \mu_0 \mathbb{1}_{u \geq X(y,1)} N(X(-y, u)) \Phi(X(-y, u)) J(-y, u)] \frac{|h(t, u)|}{N(u)} dx.
\end{aligned}$$

Combining this inequality and (43), we get

$$\begin{aligned}
&\frac{d}{dt} \int_1^b |h(t, x)| \Phi(x) dx \\
&\leq -\mu_0 \int_{X(y,1)}^b \frac{|h(t, u)|}{N(u)} N(X(-y, u)) \Phi(X(-y, u)) J(-y, u) du \\
&\leq -\mu_0 \int_1^b \frac{|h(t, X(y, x))|}{N(X(y, x))} N(x) \Phi(x) dx \\
&= -\mu_0 \int_1^b \frac{|h(t-y, x)|}{N(x)} N(x) \Phi(x) dx \\
&= -\mu_0 \int_1^b |h(t-y, x)| \Phi(x) dx \\
&\leq -\mu_0 \int_1^b |h(t, x)| \Phi(x) dx, \quad \forall t \geq y,
\end{aligned}$$

using the monotonicity property. Finally, a simple integration gives the convergence result.  $\square$

**Remark 3.** In [9], the exact solution of the problem is calculated explicitly using Laplace's transform and some complex analysis tools. The function is then given by the formula:

$$\rho(x, t) = \frac{a}{mb^\alpha \ln b} \frac{1}{x} \sum_{k=0}^{\infty} e^{\lambda_k t} \left(1 - \frac{\ln x}{\ln b}\right)^{\lambda_k/a-1} \frac{1}{c(\lambda_k)}, \quad (45)$$

for  $1 \leq x < x_p(t)$ ,

where

$$c(\lambda_k) = \sum_{n=0}^{\infty} \frac{(-\alpha \ln b)^n}{n!(\lambda_k/a + n)^2}, \quad (46)$$

and the  $\lambda_k$ 's are the roots of:

$$\frac{1}{m} \lambda_k = \sum_{n=0}^{\infty} \frac{(\alpha \ln b)^n}{(\lambda_k/a + 1) \dots (\lambda_k/a + n)} = \mathcal{F}(\lambda_k, \alpha \ln b). \quad (47)$$

We have:

$$\exists! \lambda_0 > 0 \quad \text{such that} \quad \frac{1}{m} \lambda_0 = \mathcal{F}(\lambda_0, \alpha \ln b). \quad (48)$$

In fact,  $\lambda \mapsto \mathcal{F}(\lambda, \alpha \ln b)$  is decreasing on  $\mathbb{R}^+$  and verify

$$\mathcal{F}(0, \alpha \ln b) = b^\alpha \quad \text{and} \quad \lim_{\lambda \rightarrow \infty} \mathcal{F}(\lambda, \alpha \ln b) = 0,$$

so the intermediate value theorem shows that (47) has a unique positive root denoted  $\lambda_0$ . Then one can note that the asymptotic behavior of the solution (45) is given by the first term of the sum, corresponding to  $\lambda_0$ . We can check that it is exactly what we found previously as the asymptotic behavior (see (23) and Theorem 4.2): by multiple partial integrations we show that definitions (48) and (22) of  $\lambda_0$  are equivalent. In the same way, since (23) and  $U(0) = \lambda_0$ , we can establish the following equality giving the asymptotic behavior:

$$\mathcal{N}(x, t) = C e^{\lambda_0 t} N(x) = \frac{a}{mb^\alpha \ln b} \frac{1}{c(\lambda_0)} e^{\lambda_0 t} \frac{1}{x} \left(1 - \frac{\ln x}{\ln b}\right)^{\lambda_0/a-1}, \quad (49)$$

where  $C$  is given at (36) and  $c(\lambda_0)$  at (46). Formula (45) gives us a exponential convergence rate equal to  $e^{-(\lambda_0 - \lambda_1)t}$ .

**Remark 4.** From (47) we can deduce the behavior of the  $\mu_k = \lambda_k/a$ . Let us order them:

$$\mu_0 > 0 > \mu_1 > \mu_2 > \dots > \mu_k > \dots$$

We can show that it exists  $n_0 \in \mathbb{N}$  such that  $\max_{k \neq 0} \mu_k \leq -2n_0 + 1$  and for all  $n \geq n_0$  there are exactly two roots  $\mu_n$  et  $\mu_{n+1}$  of (47) in  $I_n = ]-2n, -2n + 1[$ . Moreover, as  $n$  tends to infinity, these roots get closer and closer from the nearest negative integer:  $\mu_n + 2n - 1 \rightarrow 0$  and  $\mu_{n+1} + 2n \rightarrow 0$ . Finally we have the general behavior of the sequence  $\mu_k$ :

$$\mu_k + 2(n_0 - 1) + k \rightarrow 0. \quad (50)$$

This will be confirmed numerically in the following part.

**5. Numerics.** In this section, we discuss numerical difficulties linked to the numerical approximation of the solution of (1)-(4) and we describe suitable remedies. Equation (1) is a conservation law and the first idea to approximate the solution is to use a Godunov scheme. But a naive implementation of this method brings no result. Indeed, without a very fine discretization, which is not affordable for the clinical data ( $b = 7.3 \times 10^{10}$ ), the solution computed that way rapidly blows up.

Furthermore, we keep in mind that we request a sharp description of the large time behavior. Hence, a more adapted strategy should be introduced, that incorporates a subtle treatment of the boundary condition.

In what follows, as detailed in the introduction we choose for  $w$  the Gompertzian law (8) and we fix

$$\beta(x) = mx^\alpha.$$

**5.1. Numerical problems linked to the equation and the boundary condition.** At first, we note that the variable  $x$  varies from 1 to  $b$  which is approximately equal to  $10^{11}$  ( $b = 7.3 \times 10^{10}$ ) that makes the use of very fine grids impossible. A change of variable is necessary and we set:

$$y = \ln \frac{b}{x}.$$

But this leads us to consider the following problem

$$\partial_t u - e^y \partial_y (\tilde{w} u) = 0,$$

$$u(y, 0) = 0,$$

$$a \ln b u(\ln b, t) = \int_0^{\ln b} mb^{\alpha+1} e^{-(\alpha+1)y} u(y, t) dy + \beta(x_p(t)),$$

where  $\tilde{w}$  is given by

$$\tilde{w}(y) = aby e^{-y},$$

which is not a conservation law anymore. This remark leads us up to consider the change of function:

$$v(y, t) = be^{-y} u(y, t),$$

and the final conservation law completed with the following initial and boundary conditions:

$$\partial_t v - \partial_y (ay v) = 0, \tag{51a}$$

$$v(y, 0) = 0, \tag{51b}$$

$$a \ln b v(\ln b, t) = \int_0^{\ln b} mb^\alpha e^{-\alpha y} v(y, t) dy + \beta(x_p(t)). \tag{51c}$$

Secondly, note that in the biological variables the boundary condition is huge compared to the average solution. As we see below, the grid we use in these variable is refined near the boundary (see Figure 1): it is adapted to capture the impact of the boundary condition on the solution.

**5.2. Numerical scheme.** We now aim at solving the system (51). Since the scales of the solution and the boundary condition are very different for small times, a low order scheme does not approach well the solution. This is why we choose to use the WENO-5 scheme.

It is a finite volume scheme of fifth-order which is based on interpolations of discrete data using polynomials. It is well known that the wider the stencil, the higher the order of accuracy of the interpolation, but this is true only if the interpolated function is smooth inside the stencil. Contrary to traditional finite volume methods, the WENO (Weighted Essentially Non-Oscillatory) scheme does not use fixed stencil interpolations; it uses a convex combination of all candidate stencils instead of the one fixed in traditional schemes. The weights depend non linearly on the smoothness of the interpolated function on each stencil. This scheme is more able than a traditional one to deal with discontinuities of the interpolated function

$u$ ; it achieves automatically high order accuracy and a non-oscillatory property near discontinuities. See [14] and [15] for more details.

We consider a regular grid in the rescaled variables:

$$0 = y_{\frac{1}{2}} < y_{\frac{3}{2}} < \cdots < y_{J-\frac{1}{2}} < y_{J+\frac{1}{2}} = \ln b.$$

The grid in the biological variables is then very fine near the incoming boundary ( $x = 1$ ), as illustrated in Figure 1.

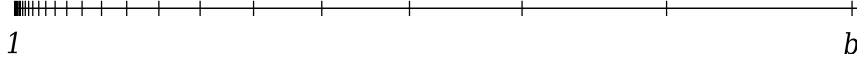


FIGURE 1. Grid displayed in the biological variables (100 points).

We define the cells and cell centers by

$$\begin{aligned} I_j &= \left[ y_{j-\frac{1}{2}}, y_{j+\frac{1}{2}} \right], \\ y_j &= \frac{1}{2} \left( y_{j-\frac{1}{2}} + y_{j+\frac{1}{2}} \right), \\ \Delta y_i &= y_{j+\frac{1}{2}} - y_{j-\frac{1}{2}} \equiv h = \frac{\ln b}{J}, \\ j &= 1, 2, \dots, J. \end{aligned}$$

Let

$$\bar{v}_j(t) = \frac{1}{\Delta y} \int_{I_j} v(y, t) dy.$$

Integrating (51) on the cell  $I_j$ , we get:

$$\frac{d}{dt} \bar{v}_j(t) - \frac{1}{\Delta y} \left[ a y_{j+\frac{1}{2}} u(y_{j+\frac{1}{2}}, t) - a y_{j-\frac{1}{2}} u(y_{j-\frac{1}{2}}, t) \right] = 0.$$

Replacing the flux  $a y_{j+\frac{1}{2}} u(y_{j+\frac{1}{2}}, t)$  with a monotone numerical flux  $\hat{f}(v_{j+\frac{1}{2}}^-, v_{j+\frac{1}{2}}^+)$  we get the semi-discretized scheme:

$$\frac{d}{dt} \bar{v}_j(t) - \frac{1}{\Delta y} \left[ \hat{f}(v_{j+\frac{1}{2}}^-, v_{j+\frac{1}{2}}^+) - \hat{f}(v_{j-\frac{1}{2}}^-, v_{j-\frac{1}{2}}^+) \right] = 0, \quad (52)$$

where  $v_{j+\frac{1}{2}}^-$  and  $v_{j+\frac{1}{2}}^+$  are approximations of the function  $v(x, t)$  at the cell boundaries.

5.2.1. *WENO reconstruction.* On each candidate stencil we reconstruct a 2nd degree polynomial  $p_i(x)$ :

$$\begin{aligned} p_2(j) &= \frac{1}{3} \bar{v}_{j-2} - \frac{7}{6} \bar{v}_{j-1} + \frac{11}{6} \bar{v}_j, \\ p_1(j) &= -\frac{1}{6} \bar{v}_{j-1} + \frac{5}{6} \bar{v}_j + \frac{1}{3} \bar{v}_{j+1}, \\ p_0(j) &= \frac{1}{3} \bar{v}_j + \frac{5}{6} \bar{v}_{j+1} - \frac{1}{6} \bar{v}_{j+2}. \end{aligned} \quad (53)$$

A WENO reconstruction will take a convex combination of the  $p_i(j)$ ,  $i \in \{0, 1, 2\}$ , defined in (53) as a new approximation of the cell boundary value  $v(x_{j+\frac{1}{2}})$ :

$$v_{j+\frac{1}{2}}^- = \sum_{r=0}^2 \omega_r p_r(j) \quad v_{j-\frac{1}{2}}^+ = \sum_{r=0}^2 \tilde{\omega}_r p_r(j-1).$$

The key of the success of WENO lies in the choice of the weights  $\omega_r$ . If the function  $v(x)$  is smooth in all the candidate stencils, one should take  $\omega_r = d_r$  with:

$$d_0 = \frac{3}{10}, \quad d_1 = \frac{3}{5}, \quad d_2 = \frac{1}{10}.$$

When the interpolated function has a discontinuity in one or more of the stencils, the corresponding weights have to be almost always 0. To measure the smoothness of the solution, we use smoothness indicators, denoted by  $\beta_i$ . The smaller this indicator  $\beta_i$ , the smoother the function in the target stencil. These  $\beta_i$  are written out explicitly as quadratic forms of the cell averages of  $v$  in the stencil:

$$\begin{aligned} \beta_2(j) &= \frac{13}{12}(\bar{v}_{j-2} - 2\bar{v}_{j-1} + \bar{v}_j)^2 + \frac{1}{4}(3\bar{v}_{j-2} - 4\bar{v}_{j-1} + \bar{v}_j)^2, \\ \beta_1(j) &= \frac{13}{12}(\bar{v}_{j-1} - 2\bar{v}_j + \bar{v}_{j+1})^2 + \frac{1}{4}(\bar{v}_{j-1} - \bar{v}_{j+1})^2, \\ \beta_0(j) &= \frac{13}{12}(\bar{v}_j - 2\bar{v}_{j+1} + \bar{v}_{j+2})^2 + \frac{1}{4}(\bar{v}_j - 4\bar{v}_{j+1} + 3\bar{v}_{j+2})^2, \end{aligned}$$

We then set the nonlinear weights:

$$\omega_r = \frac{\alpha_r}{\alpha_0 + \alpha_1 + \alpha_2}, \quad r = 0, 1, 2,$$

with

$$\alpha_r = \frac{d_r}{(\epsilon + \beta_r)^2},$$

where  $\epsilon$  is introduced to prevent the denominator from vanishing. To compute the  $\tilde{\omega}_r$  we just note that by symmetry  $\tilde{d}_r = d_{2-r}$ .

One must note that this scheme needs two additional cells on each side of the integration domain. In our method, we use ghost cells with the boundary values : an approximation of the integral (51c) at the boundary  $y = \ln b$  and 0 at  $y = 0$ .

**5.2.2. The numerical flux.** Concerning the numerical flux, we choose the following Lax-Friedrichs flux:

$$\hat{f}(v_{j+\frac{1}{2}}^-, v_{j+\frac{1}{2}}^+) = \frac{1}{2} \left[ -ay_{j+\frac{1}{2}}(v_{j+\frac{1}{2}}^- + v_{j+\frac{1}{2}}^+) - \gamma(v_{j+\frac{1}{2}}^+ - v_{j+\frac{1}{2}}^-) \right],$$

where  $\gamma = \max | -ay | = a \ln b$  is a constant.

To compute this flux, in addition to the value given by the WENO procedure, we need the value of  $v_{\frac{1}{2}}^-$  and  $v_{J+\frac{1}{2}}^+$ . We set  $v_{\frac{1}{2}}^- = 0$  and we use the boundary condition to compute  $v_{J+\frac{1}{2}}^+$ . To this end, we need a robust integration method.

5.2.3. *Integration method.* In order to compute the integral contained in the boundary condition, we use a Newton-Cotes quadrature formula. Since our WENO reconstruction is of order 5, we need an integration method of order 5 at least. This is why we use Milne's method, the Newton-Cotes quadrature method of order 5, which can be seen also as the Richardson extrapolation adapted to Simpson's method for 3 and 5 points. In order to approach the following integral:

$$I = \int_p^q f(x) dx,$$

we set  $h = \frac{q-p}{4}$ ,  $x_i = p + ih$  and  $y_i = f(x_i)$ . Then

$$J = \frac{2h}{45} (7y_0 + 32y_1 + 12y_2 + 32y_3 + 7y_4),$$

is an approximation of  $I$  of 5th-order.

Note that the Newton-Cotes method needs the value of the function at the nodes of the grid, but our method is a finite volume one. So, starting from the average value of the function on each cell we have to compute the value of the function at the nodes before computing the integral and this has to be of 5th-order. To this end, we can use again a WENO reconstruction. For the integration we set:

$$\begin{aligned} y_{\frac{1}{2}} &= v_{\frac{1}{2}}^+, \\ y_{j+\frac{1}{2}} &= \frac{1}{2} \left( v_{j+\frac{1}{2}}^+ + v_{j+\frac{1}{2}}^- \right), \quad \text{for } j = 1, \dots, J-1, \\ y_{J+\frac{1}{2}} &= v_{J+\frac{1}{2}}^-, \end{aligned}$$

where the  $v_{j+\frac{1}{2}}^+$ ,  $j = 0, \dots, J-1$ , and  $v_{j+\frac{1}{2}}^-$ ,  $j = 1, \dots, J$  are given by the WENO procedure, and we perform the integration on this vector  $y$ .

5.2.4. *Time discretization.* We use an explicit high order Runge-Kutta time discretization. The semi-discrete scheme (52) written as

$$u_t = L(u),$$

is discretized in time by the Runge-Kutta method of the third order:

$$\begin{aligned} u^{(1)} &= u^n + \Delta t L(u^n), \\ u^{(2)} &= \frac{3}{4}u^n + \frac{1}{4}u^{(1)} + \frac{1}{4}\Delta t L(u^{(1)}), \\ u^{n+1} &= \frac{1}{3}u^n + \frac{2}{3}u^{(2)} + \frac{2}{3}\Delta t L(u^{(2)}). \end{aligned}$$

**Remark 5.** As we have seen in Section 2, (51) is equivalent to the following problem:

$$\begin{cases} \partial_t v - \partial_y (ay v) = 0, \\ v(y, 0) = \delta(y = \ln b), \\ a \ln b v(\ln b, t) = \int_0^{\ln b} mb^\alpha e^{-\alpha y} v(y, t) dy. \end{cases}$$

Nevertheless, we choose to implement the first one (51), because the WENO scheme is able to deal with only one discontinuity per stencil and a Dirac approximation consists of two discontinuities on two successive cells.

### 5.2.5. Convergence analysis.

Stability. We write the stability for the Lax-Friedrichs scheme applied to (51). The scheme is described by the following recursion:

$$u_j^{n+1} = \frac{1}{2} \left( 1 + \frac{a\Delta t}{\Delta y} y_{j+1} \right) u_{j+1}^n + \frac{1}{2} \left( 1 - \frac{a\Delta t}{\Delta y} y_{j-1} \right) u_{j-1}^n,$$

$j = 1, \dots, J$ ,  $n \in \mathbb{N}$ , where  $u_j^n$  stands for the numerical approximation of  $v(t^n = n \Delta t, y_j = j \Delta y)$ . Under the CFL condition :

$$\max_{0 \leq y \leq \ln(b)} \left[ \frac{\Delta t}{\Delta y} ay \right] \leq 1,$$

we get:

$$\begin{aligned} \sum_{j=1}^J u_j^{n+1} &\leq \frac{1}{2} \left( 1 + ay_{J+1} \frac{\Delta t}{\Delta y} \right) u_{J+1}^n + \sum_{j=1}^J u_j^n, \\ &\leq \left( \sup_{0 \leq y \leq \ln b} mb^\alpha e^{-\alpha y} + 1 \right) \sum_{j=1}^J u_j^n + m(x_p(t^n))^\alpha, \\ &\leq (mb^\alpha + 1) \sum_{j=1}^J u_j^n + m(x_p(t^n))^\alpha, \end{aligned} \quad (54)$$

and using Gronwall's lemma we obtain

$$\sum_{j=1}^J u_j^n \leq e^{mb^\alpha n} \sum_{j=1}^J u_j^0 + \sum_{k=0}^{n-1} m(x_p(t^k))^\alpha e^{mb^\alpha (n-k-1)}.$$

Note that in the homogeneous case, (54) gives the  $L^1$  stability.

Consistency. Again, we write consistency for the Lax-Friedrichs scheme, and using Taylor developpement we get

$$\begin{aligned} &\left[ \frac{v(t^{n+1}, y_j) - \frac{1}{2}(v(t^n, y_{j-1}) + v(t^n, y_{j+1}))}{\Delta t} - \frac{ay_{j+1}v(t^n, y_{j+1}) - ay_{j-1}v(t^n, y_{j-1})}{2 \Delta y} \right] \\ &\quad - [\partial_t v(t^n, y_j) - \partial_y (ayv)(t^n, y_j)] \\ &= a^2 \frac{\Delta t}{2} \left( \partial_y (y \partial_y (yv)) - \frac{(\Delta y)^2}{a^2 (\Delta t)^2} \partial_{y^2}^2 v \right) + O((\Delta y)^2 + (\Delta t)^2). \end{aligned}$$

We conclude that Lax-Friedrichs scheme is of 1st-order.

Since we combine a 5th-order WENO reconstruction and a 3rd-order time discretization, we predict that our scheme is convergent of 3rd order. Numerically, we use it to compute the solution of  $\partial_t u + \partial_x u = 0$  at  $T = 1$ , for respectively a gaussian as initial condition  $u_0(x) = e^{-4x^2}$  on  $[-2; 3]$ , and  $u_0(x) = \cos(\pi x)$  on  $[-1; 1]$  with periodic boundary conditions. The numerical orders we find are respectively 5.14 and 3.92 and our previous argument validated.

**5.3. Numerical results.** In order to validate our scheme, we check that it preserves the asymptotic profile, and then we show that we can derive numerically the Malthusian rate  $\lambda_0$  from the equation. But first, for experimentation, we need to compute precisely the asymptotic profile, which means essentially to compute the first eigenvalue  $\lambda_0$  and the constant  $c(\lambda_0)$  from (47) and (46).

For the numerical tests, all the biological constants are taken from [9]:

$$a = 0.00286, \quad \alpha = 0.663, \quad b = 7.3 \times 10^{10}, \quad m = 5.3 \times 10^{-8}.$$

**5.3.1. Determination of  $\lambda_0$  and the constant  $C$  defined at (36).** In order to evaluate  $c(\lambda_0)$ , in (49), and the  $\lambda_k$ 's, we truncate the sums (46) and (47) at the numerical zero ( $\epsilon = 10^{-16}$ ) and we use the secant method to compute the  $\lambda_k$ 's. By analytic considerations, we show (see(48)) that there is only one positive root  $\lambda_0$  of (47) which is equal to

$$\lambda_0 = 5.8057 \times 10^{-3} \text{ days}^{-1}. \quad (55)$$

$\lambda_0$  can be as well determined by the integral formula (22). Since the formula defining  $c(\lambda_0)$  (see(48)) is an alternating sum, one can note that we control the rest of the sum of  $c(\lambda_0)$ 's formula (46) by the first neglected term.

**Remark 6** (In reference to Remark 4, page 18.). Using again the secant method, we can compute the following eigenvalues. More precisely, we want to confirm the asymptotic behavior of the  $\mu_k$ 's suggested in Remark 4. This is consistent with the equivalent given in (50). Numerically, we find  $n_0 = 25$  and

$$\begin{aligned} \mu_1 &= -49.239278160564048, \\ \mu_2 &= -49.8923146858060633, \\ \mu_3 &= -51.0295140700383243, \\ \mu_4 &= -51.990168667673018, \\ \mu_5 &= -53.0030304315224186, \\ \mu_6 &= -53.9990649790580122, \\ \mu_7 &= -55.000281526423727, \\ \mu_8 &= -55.9999165905830267, \\ \mu_9 &= -57.000024264683141, \\ \mu_{10} &= -57.999993061662245. \end{aligned}$$

**5.3.2. Conservation of the asymptotic profile .** We impose on our algorithm the asymptotic profile,

$$V(y) = \frac{1}{c(\lambda_0)} \frac{a}{mb^\alpha \ln b} \left( \frac{y}{\ln b} \right)^{\frac{\lambda_0}{a} - 1}, \quad (56)$$

multiplied by  $e^{-\lambda_0 t_{start}}$  as initial condition. For a value of  $t_{start}$  large enough, we expect that the solution computed by the algorithm is close to this profile (56) growing exponentially with rate  $\lambda_0$  in time. In fact, it appears that with time the integral in (51c) becomes very large compared to the source term which remains bounded, and if we neglect the source term  $\beta(x_p(t))$  in (51c), with this initial condition (56), the exact solution is

$$e^{-\lambda_0 t} b e^{-y} N(b e^{-y}),$$

since  $N(\cdot)$  is the eigenvector associated to  $\lambda_0$ , see (19a)-(19b). At time  $t_{end}$ , we compare the computed solution with

$$e^{-\lambda_0 t_{end}} b e^{-y} N(b e^{-y}),$$

(See Figure 2). For the test, we choose  $t_{start} = 10000$  days,  $t_{end} = 11000$  days.

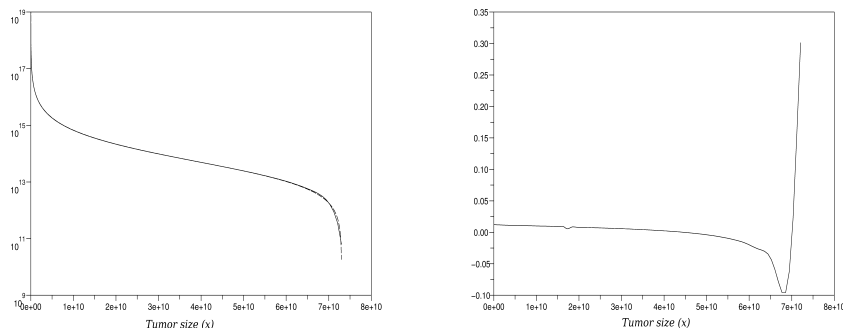


FIGURE 2. On the l.h.s, comparison between the theoretical asymptotic (dashed line) and the computed solution (log scale) and the corresponding relative error on the r.h.s. ;  
 $\alpha = 0.663$ ,  $a = 0.00286$ ,  $b = 7.3 \times 10^{10}$ ,  $m = 5.3 \times 10^{-8}$ ,  
 $t_{start} = 10000$  days,  $t_{end} = 11000$  days,  $\Delta y = \frac{\ln b}{2000}$ .

On Figure 2 we plot on the right hand side the relative error. Note that the average relative error is  $e_{err} = 2\%$  except for the larger tumors. This difference between the theoretical solution and the computed solution for large tumors can be explained by both the fact the speed  $w$  vanishes at  $x = b$  and the small number of grid nodes near  $x = b$ . However, this is exactly what we expect: the asymptotic profile is conserved and it grows at the expected Malthusian rate. Furthermore the asymptotic is conserved whether it takes into account the source term or not; it shows that this conservation property is stable under small perturbations of the boundary condition. We can also observe stability under small perturbations of the initial condition (56). All these remarks show that the scheme deals well with the non-local term in the boundary condition.

5.3.3. *The Malthusian rate.* We come back to the original problem with the initial condition (4) and the boundary condition (2). Since we showed the asymptotic behavior (35), we have

$$I(t) = \int_1^b \rho(x, t) dx \sim_{t \rightarrow +\infty} \tilde{C} e^{\lambda_0 t}.$$

We deduce from that remark that the slope of  $\ln(I)$  tends to a constant. This can be checked numerically (See Figure 3.): if we perform a linear regression on  $\ln(I(t))$  for  $4500 \leq t \leq 15000$  days, we find a slope equal to  $s = 5.8039 \times 10^{-3} \text{ days}^{-1}$  which has to be compared with (55). Let us underline that the Malthusian rate is not given by the scheme. It is a characteristic value of the problem that our scheme is able to catch. Again, this shows that our scheme computes a correct approximation of the solution, even for times larger than 10000 days.

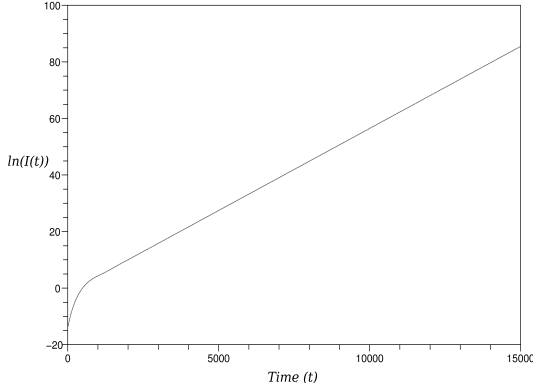
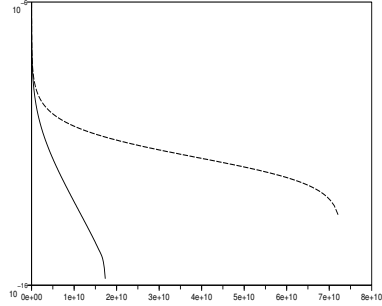


FIGURE 3.  $\ln(I(t))$  for  $0 \leq t \leq 15000$  days,  
 $\alpha = 0.663$ ,  $a = 0.00286$ ,  $b = 7.3 \times 10^{10}$ ,  $m = 5.3 \times 10^{-8}$ .

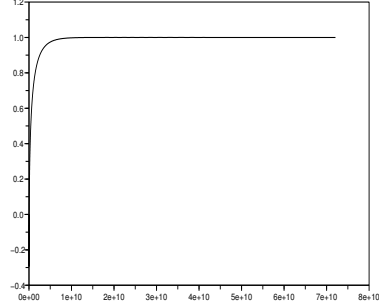
5.3.4. *Numerical asymptotic behavior.* We plot the numerical solution we obtained with our scheme for several times and we compare it with the theoretical asymptotic behavior given at (49). (See Figure 4.) Note that the behavior of the computed solution coincides with the asymptotic profile given by the theory for  $T = 5000$  days. Even for  $T = 2000$  days, the asymptotic solution is almost reached for small tumors. For the same reasons as in paragraph 5.3.2, the relative error increases again near the boundary  $x = b$ .

If we perform now the same simulation, just changing the parameter  $\alpha$  to 0.4 instead of  $\alpha = 0.663$ , we reach the U-shape profile predicted in [9]. (See Figure 5.) Again, the difference between the theoretical asymptotics and the computed solution for large tumor size can be explained by both the fact that we will always have  $\rho(b, t) = 0$ , because this tumor size is never reached (see (9)) and the small number of grid nodes near  $x = b$  (See Figure 1).

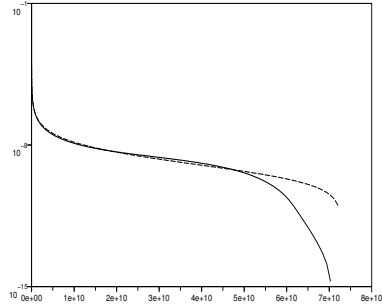
5.3.5. *Back to the generational point of view.* Intuitively, one can think that only the behaviors of the first descendants of the primary tumor may be sufficient to describe the whole dynamics. Actually this is not right. In order to illustrate it, we compute the 6 first terms of (17) and compare them to the theoretical asymptotics. If the first generations are relevant for small times, they are not anylonger after a while. (See Figure 6.) A given generation seems to be relevant only on a quite small time interval. For example, the 6-th generation has a relatively small impact on the total behavior of the system for  $t \leq 3500$  days and  $t \geq 9000$  days. Each generation has the same growth speed, however to have a relevant impact on the whole population a given generation has to wait for the previous generation to contain enough and large enough tumors to be produced. Next, since the following generation contains more tumors than the previous one (a given tumor could generate more than one malignant single cell), its weight in the whole population will become larger than the previous generation and then will generate more daughter-tumors and so on. This mechanism explains why a given generation has an impact only on a given time interval. However, if we look to the average survival time of a patient, we can consider that for applications, the first generations are relevant.



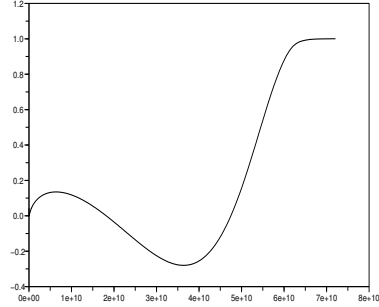
(a)  $T = 1000$  days



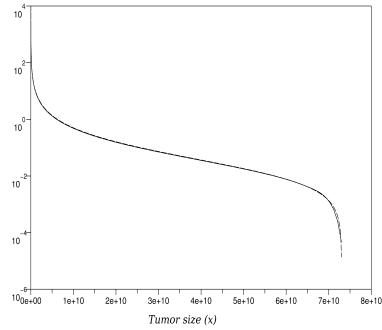
(b)  $T = 1000$  days



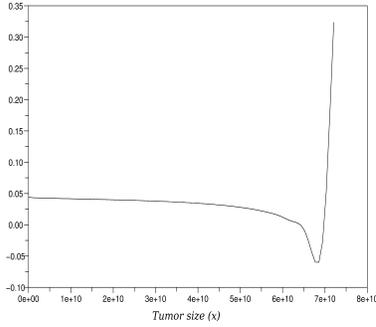
(c)  $T = 2000$  days



(d)  $T = 2000$  days



(e)  $T = 5000$  days



(f)  $T = 5000$  days

FIGURE 4. On the l.h.s, comparison between the theoretical asymptotic (dashed line) and the computed solution (log scale) and the corresponding relative error on the r.h.s. ;

$$\alpha = 0.663, a = 0.00286, b = 7.3 \times 10^{10},$$

$$m = 5.3 \times 10^{-8}, \Delta y = \frac{\ln b}{2000}.$$

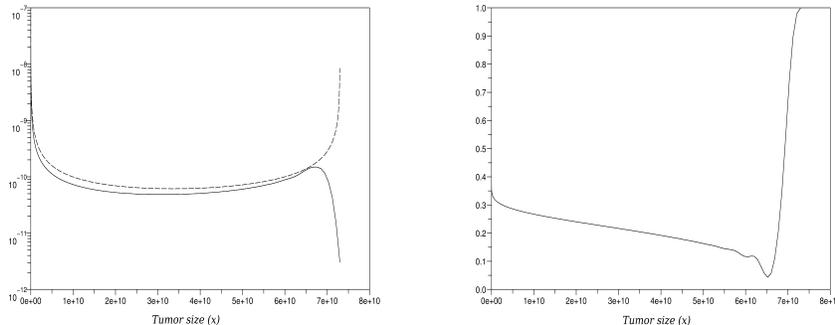


FIGURE 5. On the l.h.s, comparison between the theoretical asymptotic (dashed line) and the computed solution (log scale) and the corresponding relative error on the r.h.s. ;  $T = 5000$  days ;  
 $\alpha = 0.4$ ,  $a = 0.00286$ ,  $b = 7.3 \times 10^{10}$ ,  $m = 5.3 \times 10^{-8}$ ,  $\Delta y = \frac{\ln b}{2000}$ .

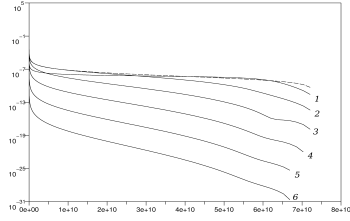
**6. Conclusion and perspectives.** Even if this model does not describe all the complexity of the biological phenomena, it brings to light the existence of a Malthusian parameter which characterizes the exponential growth of metastatic tumors and the long time asymptotics.

A straightforward finite-difference scheme cannot bring relevant results : such a scheme is not able to deal with the large boundary condition at  $x = 1$  and the solution we obtain is too large. This is why we propose here a rescaled and a high order scheme. Compared to a characteristics scheme, a strategy adopted in [1], [2], it does not need the expression of the characteristics which are explicit in this simplified model, but will not be anylonger in a more elaborate version.

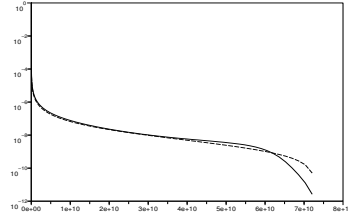
Numerically, we showed that for  $T \geq 2000$  days  $\simeq 5.5$  years, the theoretical asymptotic profile is a good approximation of the solution. However, from both a practical and a theoretical point of view, the question of the convergence speed to the asymptotic profile is still an open question.

Furthermore, this mathematical model has to be developed. For example, one has to note that no angiogenesis phenomena have been considered, but it is now well known that the tumor does not grow in the same way as before, during and after angiogenic phase of the tumor. These phenomena change the nature of the growth. See [3] for a description of the tumor growth phases.

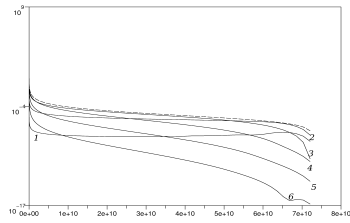
In the future, such models will be helpful for a better understanding of cancer mechanisms. They could be used as well to exhibit small tumors that medical apparatus can not detect and help designing curative strategies.



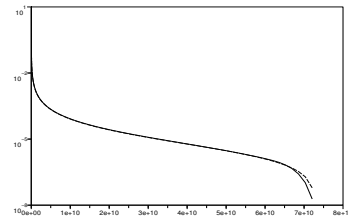
(a)  $T = 2300$  days.



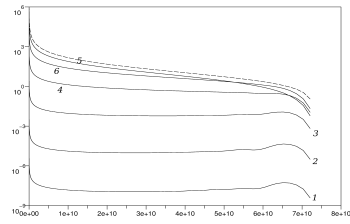
(b)  $T = 2300$  days.



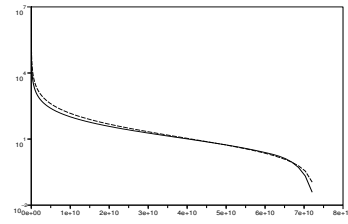
(c)  $T = 3500$  days.



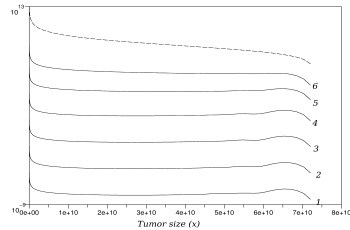
(d)  $T = 3500$  days.



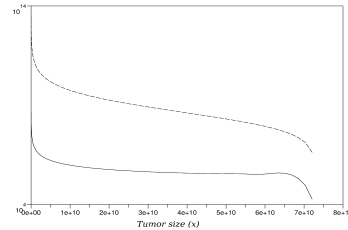
(e)  $T = 6000$  days.



(f)  $T = 6000$  days.



(g)  $T = 9000$  days.



(h)  $T = 9000$  days.

FIGURE 6. Comparison between the first 6 generations and the theoretical asymptotics (dashed line) for several times on the l.h.s and between the sum of the first 6 generations and the theoretical asymptotics (dashed line) at the same times on the r.h.s.

$$\alpha = 0.663, a = 0.00286, b = 7.3 \times 10^{10},$$

$$m = 5.3 \times 10^{-8}, \Delta y = \frac{\ln b}{2000}$$

**Appendix A. Discrete model.** From a biological point of view, a discrete model can be more understandable than a continuous one. The objective of this part is to understand the problem (15) as the limit of a discrete one. First we describe the discrete model and introduce a small parameter, then we give some estimates that are useful to pass to the limit.

**A.1. The discrete model.** We consider a model where the tumors are described by the number of cells they contain. Let  $c_i$  be the concentration of tumors containing  $i$  cells;  $c_1$  then denotes the concentration of individual tumoral cells. Obviously, we can also think of the index  $i$  as characterizing the size of the tumor. The dynamics are governed by the following assumptions:

- the tumors grow with a rate  $w_i$  that depends on the number of cells they contain. We choose for  $w_i$  a Gompertzian rate ( $w_i = a.i \ln(\frac{I}{i})$ , with  $I$  stands for the maximal tumor size and  $a$  is a constant). Note that  $w_I = 0$ .
- the tumors emit individual cells with a rate  $B_i$  depending also on the number of cells they contain: the larger this number, the larger the emitting rate. In what follows, we choose  $B_i = m.i^\alpha$ , where  $m$  is a constant and  $0 < \alpha \leq 1$ .

Accordingly, we are led to the following system of differential equations. For  $i \geq 2$ , we count the gain of tumors coming from the previous size and the loss due to the growth of the  $i$ th-tumors.

$$\frac{d}{dt}c_i = w_{i-1}c_{i-1} - w_i c_i, \quad \text{for } i \geq 2. \quad (57)$$

The evolution for the individual cells is slightly different since it counts the loss due to their own growth and the gain due to the production by all tumors; we get

$$\frac{d}{dt}c_1 = -w_1 c_1 + \sum_{i=1}^I B_i c_i. \quad (58)$$

In what follows, we aim at linking this discrete model to the continuous one (15) completed with the initial condition:

$$f|_{t=0} = f_0 \quad (59)$$

is a given function.

To rescale System (57)-(58) in terms of a small parameter, let us rewrite it in a dimensionless form. We summarize here reference quantities which will be used in the sequel:

- $T$ : the characteristic time ;
- $C_1$ : the characteristic value for the number of one-cell tumors ;
- $C$ : the characteristic value for the larger tumors,  $i \geq 2$ ;
- $B$ : the characteristic value for the emitting rates  $B_i$ ;
- $W$ : the characteristic value for the growth rates  $w_i$ .

The corresponding dimensionless quantities are defined as:

$$\bar{t} = \frac{t}{T}, \quad \bar{c}_1(\bar{t}) = \frac{c_1(\bar{t}T)}{C_1}, \quad \bar{c}_i(\bar{t}) = \frac{c_i(\bar{t}T)}{C}, \quad \bar{w}_i = \frac{w_i}{W}, \quad \bar{B}_i = \frac{B_i}{B}$$

When one rewrites (57)-(58) in terms of the new variables, the following dimensionless parameters appear:

$$\gamma = WT, \quad \text{and} \quad \kappa = \frac{BCT}{C_1}. \quad (60)$$

Omitting the overlines, the system takes the following dimensionless form:

$$\frac{d}{dt}c_i = \gamma (w_{i-1}c_{i-1} - w_i c_i), \quad (61a)$$

$$\frac{d}{dt}c_1 = -\gamma w_1 c_1 + \kappa \sum_{i=1}^I B_i c_i. \quad (61b)$$

Let us consider small tumors whose size is of  $1 + h$  order, where  $h$  is small. The dimensionless parameters defined in (60) and  $I$ , the maximal size tumor, appear as coefficients in this problem, and need to be scaled appropriately with respect to  $h$ . Let us explain the heuristics of this choice. If the right hand side of the first line of (61) is to yield a derivative, then  $\gamma$  should be scaled as the reciprocal of  $h$ . To get the equivalent to the integral in the second line,  $I$  should be scaled as  $(b - 1) = Ih$  and  $\kappa = 1$ .

More precisely, in our study, we consider that initially there are mainly small tumors of size of order  $1 + h$  and we note that then very large tumors appear only for very long times. This leads us to consider for  $T$  of order 1 only tumors which sizes are very small compared to  $I$ , the maximal size. Then these tumors “see”  $I$  as infinite and by rescaling  $I$  relatively to the size of tumors, we have  $I = (b - 1)/h$ . Finally, since we have  $\sup_i w_i = aI/e$  the previous considerations show us that  $W$  is of order  $1/h$ . These heuristic remarks lead us to the following choice of the parameters in terms of  $h$ :

$$\gamma = \frac{1}{h}, \quad \kappa = 1, \quad I = \frac{b-1}{h}.$$

With this choice of the parameters, the rescaled version of (61) is

$$\frac{d}{dt}c_i^h = \frac{w_{i-1}^h c_{i-1}^h - w_i^h c_i^h}{h}, \quad \text{for } i \geq 2 \quad (62a)$$

$$\frac{d}{dt}c_1 = -\frac{w_1^h c_1^h}{h} + \sum_{i=1}^I B_i^h c_i^h. \quad (62b)$$

where

$$h = \frac{b-1}{I},$$

$$w_i^h = a(1 + ih) \ln \left( \frac{b}{1 + ih} \right)$$

and

$$B_i^h = m(1 + ih)^\alpha, \quad 0 < \alpha \leq 1$$

In the sequel, we denote by  $f^h$  the function defined by:

$$f^h(t, x) = \sum_{i=1}^I c_i^h(t) \mathbb{1}_{ih+1 \leq x < (i+1)h+1},$$

where the  $c_i^h$ 's are solution of (62).

In what follows, we aim to establish the convergence of the rescaled discrete problem to the continuous one (15) with (59) as  $h \rightarrow 0$ . This work is inspired by [4]. After establishing *a priori* estimates, we will be able to pass to the limit in (62)

**Theorem A.1.** *Assume that there exist three constants  $M_{0,\alpha}$ ,  $M_{0,1}$ ,  $M_{0,2}$  for which  $\forall 0 < h < 1$ ,*

$$\begin{aligned} \sum_{i=1}^I m(1+ih)^\alpha c_i^h(0) &\leq M_{0,\alpha}, \\ \sum_{i=1}^I h c_i^h(0) &\leq M_{0,1}, \\ h^2 \sum_{i=0}^I i c_i^h(0) &\leq M_{0,2}, \end{aligned}$$

*Then there exists a subsequence  $h_n$  such that:*

$$\begin{aligned} f^{h_n} &\rightharpoonup f, \quad \text{in } C^0([0, T]; \mathcal{M}^1([1, b]) - \text{weak} - *), \\ f_0^{h_n} &\rightharpoonup \mu_0, \quad \text{in } \mathcal{M}^1([1, b]). \end{aligned}$$

where  $f_0^h$  is defined by

$$f_0^h(t, x) = \sum_{i=1}^I c_i^h(0) \mathbb{1}_{ih+1 \leq x < (i+1)h+1},$$

and where  $f$  is the solution of (15) with the initial condition  $f|_{t=0} = \mu_0$ .

**Remark 7.** In particular, if

$$c_i^h(0) = \frac{1}{h} \int_{1+ih}^{1+(i+1)h} f_0(y) dy$$

for a given function  $f_0 \in L^1([1, b])$  then  $f_0^h \rightarrow f_0$  in  $L^1([1, b])$  and

$$f^h \rightharpoonup f, \quad \text{in } C^0([0, T]; L^1([1, b]) - \text{weak} - *).$$

since we showed that the solution of (15) with a given initial condition is unique.

**A.2. Estimates.** In this first section we will prove some estimates we will use further on. Note that as a consequence of (57)-(58), we obtain the following relation for the evolution of the total number of tumors

$$\frac{d}{dt} \sum_{i=1}^I c_i^h = \sum_{i=1}^I B_i^h c_i^h.$$

More generally, for any sequence  $\varphi_i$ , we get the following weak formulation:

$$\sum_{i=1}^I \varphi_i c_i^h(t) = \sum_{i=1}^I \varphi_i c_i^h(0) + \int_0^t \sum_{i=1}^I \frac{w_i^h c_i^h}{h} (\varphi_{i+1} - \varphi_i) ds + \int_0^t \varphi_1 \sum_{i=1}^I B_i^h c_i^h ds. \quad (63)$$

Let us at first choose  $\varphi_i = (1+ih)^\alpha$ . Since  $0 < \alpha \leq 1$ , we have:

$$0 \leq \varphi_{i+1} - \varphi_i \leq h\alpha(1+ih)^{\alpha-1}.$$

Then, now using (63):

$$\begin{aligned}
& \sum_{i=1}^I m(1+ih)^\alpha c_i^h(t) \\
& \leq m \sum_{i=1}^I (1+ih)^\alpha c_i^h(0) + \int_0^t m \sum_{i=1}^I a(1+ih) \ln\left(\frac{b}{1+ih}\right) c_i^h(s) \alpha (1+ih)^{\alpha-1} ds \\
& \quad + m \int_0^t (1+h)^\alpha \sum_{i=1}^I m(1+ih)^\alpha c_i^h(s) ds, \\
& \leq m \sum_{i=1}^I (1+ih)^\alpha c_i^h(0) + \int_0^t (a\alpha \ln b + 2m) \sum_{i=1}^I m(1+ih)^\alpha c_i^h(s) ds,
\end{aligned}$$

(recall that  $h \leq 1$ ), i.e.

$$\sum_{i=1}^I B_i^h c_i^h(t) \leq mM_{0,\alpha} + \int_0^t (a\alpha \ln b + 2m) \sum_{i=1}^I B_i^h c_i^h(s) ds$$

Using Gronwall's lemma, we get

$$\sup_{0 \leq t \leq T} \sum_{i=1}^I B_i^h c_i^h(t) \leq M_B, \tag{64}$$

where  $M_B$  does not depend on  $h$ .

We can now estimate the moments:

• **0th-order moment:** We have:

$$\begin{aligned}
\int_1^b f^h(t, x) dx &= h \sum_{i=1}^I c_i^h(t) \\
&= \int_0^t h \sum_{i=1}^I B_i^h c_i^h(s) ds + \sum_{i=1}^I h c_i(0) \\
&\leq TM_B + M_{0,1} \leq M^0,
\end{aligned}$$

Finally we get:

$$\sup_{0 \leq t \leq T} \int_1^b f^h(t, x) dx \leq M^0,$$

where  $M^0$  does not depend on  $h$ .

- **1st-order moment:** We have:

$$\begin{aligned}
\int_1^b x f^h(t, x) dx &= \sum_{i=1}^I \int_{ih+1}^{(i+1)h+1} x c_i^h(t) dx \\
&= h^2 \sum_{i=1}^I i c_i^h(t) + \left(\frac{h^2}{2} + h\right) \sum_{i=1}^I c_i(t) \\
&= S_1 + S_2.
\end{aligned}$$

$S_2$  is bounded by  $2M^0$  and we have:

$$\begin{aligned}
S_1 &= h^2 \int_0^t \sum_{i=1}^I \frac{w_i^h c_i^h(s)}{h} ds + \int_0^t h^2 \sum_{i=1}^I B_i^h c_i^h(s) ds + h^2 \sum_{i=0}^I i c_i^h(0) \\
&\leq TM_B + M_{0,2} + h^2 \int_0^t \sum_{i=1}^I \frac{1}{h} a(ih+1) \ln\left(\frac{b}{ih+1}\right) c_i^h(s) ds \\
&\leq TM_B + M_{0,2} + a \ln b \int_0^t \sum_{i=1}^I h^2 i c_i^h(s) ds + a \ln b h \int_0^t \sum_{i=1}^I c_i^h(s) ds \\
&\leq TM_B + M_{0,2} + a \ln b \int_0^t h^2 \sum_{i=1}^I i c_i^h(s) ds + Ta \ln b M^0 \\
&\leq C + a \ln b \int_0^t h^2 \sum_{i=1}^I i c_i^h(s) ds.
\end{aligned}$$

Using again Gronwall's lemma we get:

$$\sup_{0 \leq t \leq T} \int_1^b x f^h(t, x) dx \leq M^1,$$

where  $M^1$  does not depend on  $h$ .

**A.3. Proof of Theorem A.1.** Let  $\varphi$  be a smooth function ( $\varphi \in \mathcal{C}^1$ ) supported in  $[1, b]$ . We set

$$\varphi^h(x) = \varphi(x_i) \quad \text{for } x_i = ih + 1 \leq x < (i+1)h + 1.$$

Note that  $\varphi^h$  converges uniformly to  $\varphi$  on  $[1, b]$ .

We fix  $\varphi_i = h \varphi(ih + 1)$  in (63). Therefore, we obtain:

$$\begin{aligned} \sum_{i=1}^I h\varphi(ih + 1)c_i^h(t) &= \sum_{i=0}^I h\varphi(ih + 1)c_i^h(0) \\ &+ \int_0^t \sum_{i=1}^I \frac{w_i c_i^h(s)}{h} (h\varphi((i + 1)h + 1) - h\varphi(ih + 1)) ds \\ &+ \int_0^t h\varphi(h + 1) \sum_{i=1}^I B_i^h c_i^h(s) ds, \end{aligned}$$

which is equivalent to :

$$\begin{aligned} &\int_1^b f^h(t, x)\varphi^h(x) dx - \int_1^b f^h(0, x)\varphi^h(x) dx \\ &= \int_0^t \int_1^b w^h(x)f^h(\sigma, x)\Delta\varphi^h(x) dx d\sigma \\ &+ \int_0^t \varphi(h + 1) \int_1^b B^h(x)f^h(\sigma, x) dx d\sigma, \end{aligned} \tag{65}$$

where we have set

$$\Delta\varphi^h(x) = \frac{\varphi^h(x + h) - \varphi^h(x)}{h}.$$

It is straightforward to check that as  $h \rightarrow 0$ , the quantity  $\Delta\varphi^h$  converges uniformly to  $\varphi'$  on  $[1, b]$ .

Since  $w^h(x)$  is bounded by  $(a \ln b)x$  for any  $x$  in  $[1, b]$  and we have the upperbound (64), (65) leads to

$$\left| \int_1^b f^h(t_1, x)\varphi^h(x)dx - \int_1^b f^h(t_2, x)\varphi^h(x)dx \right| \leq (Cst. \|\varphi'\|_\infty M^1 + M_B \|\varphi\|_\infty) |t_1 - t_2|$$

which proves that  $\left( t \mapsto \int_1^b f^h(t, x)\varphi^h(x)dx \right)_{h \geq 0}$  is equicontinuous on  $[0, T]$ . It is also equibounded:

$$\left| \int_1^b f^h(t, x)\varphi^h(x)dx \right| \leq \|\varphi\|_\infty M^0.$$

Therefore, by the Ascoli theorem it belongs to a compact set of  $\mathcal{C}^0([0, T])$ .

Moreover, since  $\varphi^h$  approaches  $\varphi$  uniformly on  $[1, b]$ , one deduces that the sequence  $\left( t \mapsto \int_1^b f^h(t, x)\varphi(x)dx \right)_{h \geq 0}$  lies in a compact set of  $\mathcal{C}^0([0, T])$ .

Let  $\varphi$  be in  $\mathcal{C}_b^0([1, b])$ , then by separability, there exists a sequence  $\varphi_k$  of functions in  $\mathcal{C}^1([1, b])$  such that  $\varphi_k \rightarrow \varphi$ . By the diagonal Cantor process, we can find subsequences,  $h_n$  and  $k_n$ , and  $f \in \mathcal{C}^0([0, T], \mathcal{M}^1([1, b]) - \text{weak} - *)$  such that

$$\int_1^b \varphi_{k_n} f^{h_n} dx \rightarrow \int_1^b \varphi(x) f(t, dx).$$

But

$$\left| \int_1^b (\varphi - \varphi_{k_n}) f^{h_n}(t, x) dx \right| \leq \|\varphi - \varphi_{k_n}\| M^0,$$

Hence, we can find a subsequence, labeled  $h_n$ , and a function  $f$  that belongs to  $\mathcal{C}^0([0, T], \mathcal{M}^1([1, b]) - \text{weak} - *)$  such that the following convergence

$$\int_1^b \varphi(x) f^{h_n}(t, x) dx \rightarrow \int_1^b \varphi(x) f(t, dx)$$

as  $h_n$  tends to 0, holds uniformly on  $[0, T]$ , for any  $\varphi \in \mathcal{C}_b^0([1, b])$  and any  $T > 0$ .

Now, we are able to pass to the limit in (65). Since  $w$  and  $B$  are regular,  $w^{h_n}$  and  $B^{h_n}$  converge uniformly to  $w$  and  $B$  respectively on  $[1, b]$ . Then, we get for any  $\varphi \in \mathcal{C}_b^0([1, b])$ :

$$\begin{aligned} \int_1^b f(t, x) \varphi(x) dx - \int_1^b f(0, x) \varphi(x) dx &= \int_0^t \int_1^b w(x) f(\sigma, x) \varphi'(x) dx d\sigma \\ &+ \int_0^t \varphi(1) \int_1^b B(x) f(\sigma, x) dx d\sigma, \end{aligned}$$

which correspond to the weak formulation of (15) with (59). In particular, at  $t = 0$ , the limit  $f(t = 0, x)$  is given by the limit of  $f^{h_n}(0, x)$  built from the  $c_i^{0, h_n}$ . This completes the proof of the theorem.

**Acknowledgments.** We thank D. Barbolosi who pointed us Ref. [9] and introduced us to the problem. During the preparation of this work we learnt a lot from many fruitful discussions with B. Perthame, J. Clairambault and E. Grenier. We thank also P. Michel for his fruitful remarks. We are also gratefully indebted to A. Ben Abdallah, F. Hubert and F. Verga for friendly exchanges on the different approaches to the problem.

## REFERENCES

- [1] Oscar Angulo and J. C. López-Marcos, *Numerical schemes for size-structured population equations*, Math. Biosci., **157** (1999), 169–188. Deterministic models with applications in population dynamics and other fields of biology (Sofia, 1997).
- [2] Dominique Barbolosi, Assia Benabdallah, Florence Hubert and Federico Verga, *Mathematical and numerical analysis for a model of growing metastatic tumors*, Math. Biosci., **218** (2009), 1–14.
- [3] Nicola Bellomo and Luidgi Preziosi, *Modelling and mathematical problems related to tumor evolution and its interaction with the immune system*, Math. Comput. Modelling, **32** (2000), 413–452.
- [4] Jean-Francois Collet, Thierry Goudon, Frédéric Poupaud and Alexis Vasseur, *The Becker-Döring system and its Lifshitz-Slyozov limit*, SIAM J. Appl. Math., **62** (2002), 1488–1500 (electronic).
- [5] C. L. Frenzen and J. D. Murray, *A cell kinetics justification for Gompertz' equation*, SIAM J. Appl. Math., **46** (1986), 614–629.
- [6] Piotr Gwiazda and Benoît Perthame, *Invariants and exponential rate of convergence to steady state in the renewal equation*, Markov Process. Related Fields, **12** (2006), 413–424.
- [7] Mats Gyllenberg and Glenn F. Webb, *A nonlinear structured population model of tumor growth with quiescence*, J. Math. Biol., **28** (1990), 671–694.
- [8] Mats Gyllenberg and Glenn F. Webb, *Quiescence as an explanation of gompertzian tumor growth*, Growth Development & Aging, **53** (1989), 25–33.

- [9] K. Iwata, K. Kawasaki and N. Shigesada, *A dynamical model for the growth and size distribution of multiple metastatic tumors*, Journal of Theoretical Biology, **203** (2000), 177–186.
- [10] Frank Kozusko and Željko Bajzer, *Combining Gompertzian growth and cell population dynamics*, Math. Biosci., **185** (2003), 153–167.
- [11] Philippe Michel, *Principe d'entropie généralisée et dynamique de populations structurées*, Thèse de doctorat, Université Paris IX-Dauphine, november 2005.
- [12] Philippe Michel, Stéphane Mischler and Benoît Perthame, *General entropy equations for structured population models and scattering*, C. R. Math. Acad. Sci. Paris, **338** (2004), 697–702.
- [13] Benoît Perthame, *Transport equations in biology*, Frontiers in Mathematics. Birkhäuser Verlag, Basel, 2007.
- [14] Giovanni Russo, “High Order Shock Capturing Schemes for Balance Laws,” In “Numerical Solutions of Partial Differential Equations,” pages 160–251, Advanced Courses in Mathematics - CRM Barcelona. Basel: Birkhäuser., 2009.
- [15] Chi-Wang Shu, “Essentially Non-oscillatory and Weighted Essentially Non-oscillatory Schemes for Hyperbolic Conservation Laws,” In “Advanced Numerical Approximation of Nonlinear Hyperbolic Equations” (Cetraro, 1997), volume **1697** of Lecture Notes in Math., 325–432, Springer, Berlin, 1998.

Received July 2008; revised July 2009.

*E-mail address:* `anne.devys@inria.fr`

*E-mail address:* `thierry.goudon@inria.fr`

*E-mail address:* `pauline.lafitte@math.univ-lille1.fr`